arXiv:1407.6504v4 [nucl-th] 30 Oct 2014

Electron Capture in ^{163}Ho, Overlap plus Exchange Corrections and the Neutrino Mass.

Amand Faessler[1], Loredana Gastaldo[2], F. Šimkovic[3],

[1]Institute of Theoretical Physics, University of Tuebingen, Germany
[2]Kirchhoff Institut für Physik, University of Heidelberg, Germany
[3]JINR, 141980 Dubna, Moscow Region, Russia and
Comenius University, Physics Dept., $SK-84215$ Bratislava, Slovakia.

October 31, 2014

Abstract

Holmium 163 offers perhaps the best chance to determine the neutrino mass by electron capture. This contribution treats the electron capture in $^{163}Holmium$ completely relativistic for the overlap and exchange corrections and the description of the bolometer Spectrum. The theoretical expressions are derived consistently in second quantization with the help of Wick's theorem assuming single Slater determinants for the initial Ho and the final Dy atoms with holes in the final $ns_{1/2}$ and $np_{1/2}$ states. One needs no hand waving arguments to derive the exchange terms. It seems, that for the first time the multiplicity of electrons in the orbital overlaps are included in the numerical treatment. Electron capture $e^- + p \to n + \nu_e$ is proportional to the probability to find the captured electron in the parent atom at the nucleus. Non-relativistically this is only possible for $ns_{1/2}$ electron states. Relativistically also $p_{1/2}$ electrons have a probability due to the lower part of the relativistic electron spinor, which does not disappear at the origin. Moreover relativistic effects increase by contraction the electron probability at the nucleus. Capture from other states are suppressed. However they can be allowed with smaller intensity due to finite nuclear size. These probabilities are at least three orders smaller than the electron capture from $3s_{1/2}$ and $3p_{1/2}$ states. The purpose of this work is to give a consistent relativistic formulation and treatment of the overlap and exchange corrections for electron capture in $^{163}_{67}Ho$ to excited atomic states in $^{163}_{66}Dy$ and to show the influence of the different configurations in the final Dy states. The overlap and exchange corrections are essential for the calorimetric spectrum of the deexcitation of the hole states in Dysprosium. The slope of the upper end of the spectrum, which contains the information on the electron neutrino mass, is different. In addition the effect of the finite energy resolution on the spectrum and on the determination of the neutrino mass is studied. The neutrino mass must finally be determined by maximum likelihood methods to fit the theoretical spectra at the upper end near the Q value varying the neutrino mass, the Q-value and probably also the energy resolution, because at the moment Q and the energy resolution are not known to the accuracy needed.

1 Introduction

Neutrino oscillations give the differences of the mass eigenvalue m_i $(i = 1,\ 2, 3)$ squared, but they cant determine the absolute value of the neutrino mass eigenstates. The Tritium beta decay gives for

direct determinations presently the best upper limit of about 2.2 [eV] for the anti-electron neutrino mass [1, 2, 4]. In the future one expects, that this value will be improved by the KATRIN experiment [4]. The electron Majorana neutrino mass can be determined by the neutrinoless double beta decay [5, 6, 7]. The electron neutrino mass can also be obtained by electron capture on a proton in nuclei [8, 9, 10, 11, 14, 32].

$$p + e^- \rightarrow n + \nu_e \tag{1}$$

For electron capture the decay ${}^{163}_{67}Ho_{96} \rightarrow {}^{163}_{66}\ Dy_{97}$ seems to be the most promising case due to the small Q-value between 2.3 [keV] [12] and 2.8 [keV] [10, 13, 22] with a recommended value of $Q = (2.55 \pm 0.016)\ keV$ [15].

$$Q = M(^{163}Ho) - M(^{163}Dy) \approx 2.5keV \tag{2}$$

In the electron capture process one can distinguish two steps [16]. First the electron is captured in the state $|k>$ in ^{163}Ho, an electron neutrino is emitted with energy E_ν and an excited state is formed in ^{163}Dy with a hole in the electron orbital $|f'>$ with the same quantum numbers as $|f>$ in ^{163}Ho. A calorimetric measurement "detects" the total energy of the second step plus the nuclear recoil occurring in the first stage, which is of the order of meV and will be neglected in the following discussion. The other and major part of the energy released during the first step is carried away unmeasured by the electron neutrino. The excited atomic hole states in Dy decay into the ground state emitting either electrons or/and photons. A bolometric (calorimetric) measurement obtains the total energy of this second decay. The spectrum measured by the bolometer in the second step is given by the incoherent sum over the final hole states in Dy [16].

$$\frac{d\Gamma}{dE_c} \propto (Q - E_c)\sqrt{(Q - E_c)^2 - m_\nu^2} \sum_{f=f'} \lambda_0 B_f \frac{\Gamma_{f'}}{2\pi} \frac{1}{(E_c - E_{f'})^2 + \Gamma_{f'}^2/4} \tag{3}$$

The quantity λ_{f0} contains the nuclear matrix element and is defined in eq. (8). The total energy available for the decay, Q, is divided in the first step into the excitation energy E_c of ^{163}Dy and the energy of the emitted neutrino $E_\nu = \sqrt{m_\nu^2 + p_\nu^2}$. The excitation energy of Dy is then:

$$E_c = Q - E_\nu \ \ and \ \ E_c(max) = \lim_{p_\nu \rightarrow 0} E_c = Q - m_\nu \tag{4}$$

So the upper end of the decay spectrum in the calometric measurement is for all excitations of ^{163}Dy the same. The maximum available energy for the sum of the secondary processes (X-ray decay, Auger electron emission) measured by the bolometer is $E_c = Q - m_\nu$. This allows to determine the electron neutrino mass from electron capture due to a suppression of counts around the interval $< Q - m_\nu\ ,\ Q >$ [10, 28]. Since the finite neutrino mass is a very minor effect on the calorimetric spectrum, not only a very precise Q value must be determined, but one needs also, since the energy resolution is limited, the form of the spectrum at the upper end accurately. The purpose of the present work is to determine this spectrum and the effect of a finite neutrino mass on the spectrum, so that one has a chance to determine the mass of the electron neutrino. Among other effects we will show, that the bolometer spectrum depends sensitively on the overlap and exchange corrections. They determine the relative contributions of the excited hole states in ^{163}Dy on the spectrum. To study these effects is one of the purposes of this work.

The sum f = f' in eq. (3) runs in principle over all occupied s and $p_{1/2}$ electron levels in Holmium (see table 1). Due to energy conservation the sum is constraint to states $3s_{1/2}$ and $3p_{1/2}$ and higher. The sum runs also correlated over f' the hole states in Dy with $|f'> = |n,\ \ell,\ j> = |f>$ as a single sum over states with the same quantum numbers. The reasons is that the captured electron in Ho must have for the leading overlap term the same quantum numbers as the hole in Dy. Contributions

with $f \neq f'$ are quadratic in the small "non-diagonal" overlaps (see table 2) and are neglected. $E_{f'}$ and $\Gamma_{f'}$ are the energies and the width of the hole states in ^{163}Dy given in eq. (26). The overlap and exchange correction B_f is defined in eq. (20) and includes a sum over the capture states in Holmium $i = 1s,\ 2s,\ 3s,\ 4s,\ 5s,\ 6s$ and $2p_{1/2},\ 3p_{1/2},\ 4p_{1/2},\ 5p_{1/2}$ (see table 1). But as already mentioned due to energy conservation the sum for captured electrons in ^{163}Ho is restricted to $3s_{1/2}$ and to $3p_{1/2}$ and higher. All energy allowed occupied s and $p_{1/2}$ levels in Ho are included in this work.

The effective anti-neutrino mass m_β measured in the Tritium decay and the neutrino mass to be measured in electron capture is given by

$$\begin{aligned} m_\beta &= \sqrt{\sum_{k=1}^{3} |U_{ek}|^2 m_k^2} \\ &\approx m_\nu. \end{aligned} \tag{5}$$

The last approximate equal sign is obtained under the assumption $m_\nu \approx m_1 \approx m_2 \approx m_3$.

The neutrinoless double beta decay [5, 7, 11] determines the effective Majorana neutrino mass:

$$| < m_{\beta\beta} > | = |m_1|U_{e1}|^2 + m_2|U_{e2}|^2 \cdot e^{i\alpha_{21}} + m_3|U_{e3}|^2 \cdot e^{i\alpha_{31}}| \tag{6}$$

Here the angles α_{21} and α_{31} yield the Majorana phases $e^{i\alpha}$. For a time reversal symmetric theory they must be real and can have the values ± 1 only. The coefficients U_{ej} of the Pontecorvo-Maki-Nakagawa-Sakata mixing matrix describe the transformation from mass ν_1, ν_2, ν_3 to flavor eigenstates ν_e, ν_ν, ν_τ of the neutrinos.

$$\begin{pmatrix} \nu_e \\ \nu_\mu \\ \nu_\tau \end{pmatrix} = \begin{pmatrix} U_{e1} & U_{e2} & U_{e3} \\ U_{\mu 1} & U_{\mu 2} & U_{\mu 3} \\ U_{\tau 1} & U_{tau2} & U_{\tau 3} \end{pmatrix} \begin{pmatrix} \nu_1 \\ \nu_2 \\ \nu_3 \end{pmatrix} \tag{7}$$

2 Description of Electron Capture

The details of the evaluation of the electron capture probability are given by Bambynek et al. [17]. λ_{f0} is the electron capture probability assuming a complete identity and orthonormality between the electron states of the parent nucleus ($^{163}Holmium$) and of the daughter nucleus ($^{163}Dysprosium$). In our case:

$$\lambda_0 \propto G^2 \xi |\psi_{3s1/2}(R)|^2 \tag{8}$$

G is the weak Fermi coupling constant, ξ the nuclear matrix element squared and $\psi_{3s1/2}(R)$ is the lowest energetically allowed single electron wave function of the parent at the nuclear radius (see table 1) for the capture process of eq. (1). The radial part of the spinor wave function is defined and normalized as:

$$\begin{aligned} \psi_A(r) &= \frac{1}{r} \begin{pmatrix} P_A \\ Q_A \end{pmatrix} \\ < A|B > &= \int_{0,\infty} \Big(P_A(r) \cdot P_B(r) + Q_A(r) \cdot Q_B(r) \Big) \cdot dr = \delta_{A,B} \end{aligned} \tag{9}$$

The overlap of wave functions with the quantum numbers $|A >= |n, \ell, j >$ in the parent atom and the quantum numbers $|B' >= |n', \ell, j >$ in the daughter is given by (see table 2):

$$< A|B' >= \int_{0,\infty} \Big(P_A(r) \cdot P_{B'}(r) + Q_A(r) \cdot Q_{B'}(r)\Big) \cdot dr = overlap(A, B') \tag{10}$$

Until now the probability of electron capture was normally calculated with the captured electron wave function at the origin for $P_{ns}(r)$ and $Q_{np1/2}(r)$. All the other electron wave functions disappear at $r = 0$. In reality the wave functions have to be integrated in the nuclear matrix element over the nucleus. In almost all previous calculations these wave functions of the captured electrons are taken at the origin. In the present work as a better approximation the upper spinor amplitude for capture from the states $ns_{1/2}$ and the lower amplitude for capture from the $np_{1/2}$ levels in Holmium are taken at the nuclear radius (11). The finite size of the nucleus allows with reduced probabilities also capture from other than $ns_{1/2}$ and $np_{1/2}$ states (see table 5).

$$R = 1.2 \cdot A^{1/3}\ [fm] = 2.2676 \cdot 10^{-5} A^{1/3}\ [au] \rightarrow 1.2386 \cdot 10^{-4}\ [au] \quad for Ho; \tag{11}$$

We assume, that the total atomic wave function can be described by a single Slater determinant. B_f in eq. (3) takes into account the overlaps and the exchange terms between the parent $|G>$ and the daughter atom in the state $|A'_f>$ with a hole in the electron state $|f'>$.

$$B_f = |\sum_i \psi_i(R) < A'_f|a_i|G > |^2 / |\psi_{3s1/2}(R)|^2 \tag{12}$$

Here $\psi_f(R) = P_{ns1/2}(R)/R$ or $Q_{np1/2}(R)/R$ are electron wave functions at the nuclear radius in the parent state (9), which have the largest overlaps (10) with the final electron hole states in the daughter nucleus. In eq. (12) one has to divide out the wave function of the captured electron in Holmium $|\psi_i(R)|^2$ from eq.(8) contained in eq. (3). The sum i in eq.(12) runs over the occupied and energetically allowed $3s,\ 4s,\ 5s,\ 6s$, and $3p_{1/2},\ 4p_{1/2},\ 5p_{1/2}$, electrons states in ^{163}Ho. Due to energy conservation only captures of $3s_{1/2}$ and $3p_{1/2}$ states and higher are allowed.

One assumes generally, that the initial $|G>$ and final $|A'_f>$ atomic wave functions can be given as Slater determinants. They are in this work calculated selfconsistently with a hole in state i in eq. (12) and with a single Slater Determinant Dirac-Fock code developed by Grant [18] and modified by Desclaux [19] and Ankudinov et al. [20].

Configuration mixing affects mostly the valence electrons, while electron capture (EC) involves mainly the inner electrons. Thus a representation of wave functions by Slater determinants should be a good description for the EC process. But configuration mixing could lead to small satellite lines. The Slater wave functions of the initial Holmium in the ground state $|G>$ and the excited electron hole states $|A'_f>$ in Dysprosium read in second quantization:

$$|G >= a_1^\dagger a_2^\dagger a_3^\dagger ... a_Z^\dagger |0> \tag{13}$$

$$|A'_f >= a_1'^\dagger a_2'^\dagger ... a_{f-1}'^\dagger a_{f+1}'^\dagger ... a_Z'^\dagger |0> \tag{14}$$

The primes' indicate the single electron spinor creation operators for the daughter nucleus (Dysprosium) with an electron hole in the single particle state $|f'>$. The following expression has to be calculated with the help of Wick's theorem [21].

$$\sum_i \psi_i(R) < A'_f|a_i|G >= \sum_i \psi_i(R) \cdot < 0|a'_Z a'_{Z-1} ... a'_{f+1} a'_{f-1} ... a'_1 \cdot a_i \cdot a_1^\dagger a_2^\dagger a_3^\dagger ... a_Z^\dagger |0> \tag{15}$$

In eq.(15) and also in later expressions for capture from Holmium $s_{1/2}$ states the upper spinor components $P_{ns1/2}(R)/R$ and for capture from $p_{1/2}$ states the lower spinor components $Q_{np1/2}(R)/R$ are taken for $\psi_i(R)$ at the nuclear radius (11) in Holmium. The vacuum expectation value in eq. (15) has

now to be fully Wick contracted [21]. Although the single electron wave functions are different for the parent (Holmium) and the daughter atom (Dysprosium) with a hole in $|f'>$, the corresponding electron states $|k>$ in the parent and $|k'>$ in the daughter with the same quantum numbers $|n,\ell,j>$ have still the largest overlap (10) (see table 2). Contractions $<k'|m>$ with radial quantum numbers n_m and $n'_{k'}$ different are small. The overlaps of parent and daughter states with different ℓ and j are zero. We neglect all terms with two or more such small single particle overlaps $<n',\ell,j|n,\ell,j>$. In case one obtains several large non-diagonal $n \neq n'$ overlaps, such higher order terms must be included according to the vacuum expectation value (15) with Wick's [21] theorem. But the non-diagonal overlaps are normally about two or even three orders of magnitude smaller and quadratic terms in these small quantities can be neglected. The maximum value of all the non-diagonal overlaps is $<3s'|4s>=0.023$. At this point one can already conclude, that the probability to excite two holes in the ^{163}Dy atom is less than 10^{-3} smaller, than exciting only one hole. A detailed discussion is given in the next section (See eq. (18).)

$$F_{0f} = \psi_f(R)(-)^{f+1} \prod_{k\neq f} < k'|k > \tag{16}$$

$$F_f = \sum_b \psi_b(R) < A'_f|a_b|G > \approx \sum_{b=1\ldots Z} \psi_b(R)[(-)^{f+1}\delta_{b,f} \prod_{k\neq f} < k'|k > + (-)^f \delta_{b\neq f} < b'|f > \prod_{k\neq(f,b)} < k'|k >] \tag{17}$$

The index b runs over the states i from eq. (15), from which the electrons are captured. The amplitudes F_{0f} and F_f are listed in table 3. If one wants to include the final excited daughter atom Holmium with two holes in f_1 and f_2 and an additional occupied electron state c, which can be a bound or a continuum state, one must add to the amplitude F_f the amplitude (18).

$$F_f(2\ holes) = \sum_b \psi_b(R) < A'_f(2\ holes)|a_b|G > \approx \sum_{b=1\ldots Z} \psi_b(R)(-)^{f_2-f_1+Z} \cdot[< b'|f_1 >< c'|f_2 > - < b'|f_2 >< c'|f_1 >] \cdot \prod_{k=1..Z\neq(f_1,f_2,b)} < k'|k > \tag{18}$$

Here again k and k' and also b and b' stand for the same quantum numbers in the parent and the daughter atom. The sum over b runs also over b'. If c is a continuum state (correctly normalized) one speaks of 'shake off' into the continuum. Since now two "non-diagonal" overlaps are involved in eq. (18) with $<b'|f_1>$ and $<c'|f_2>$ and the corresponding exchange term interchanging f_1 and f_2 with a minus sign, this probability is by more than a factor 10^{-3} smaller as mentioned already above (for the overlap amplitudes see table 2) and is neglected. This expression is here for the first time given analytically. Eq. (17) and (18) describe the first step of the electron capture process, where the energy is carried away by the neutrino. The deexcitation of the hole or the two holes states in the second step can be measured using micro-calorimeters, as has been demonstrated by ECHo [8, 9, 10, 22, 32]. The hole states in ^{163}Dy deexcite due to X rays (smaller probabilities for the smaller transition energies in outer shells), Auger transitions (increasing contributions for outer shells) and Coster-Kronig transitions [16]. The energy release in the first step by the neutrino escapes detection.

Using eqs. (16) and (17) one can calculate the overlap and exchange corrections for eq. (3).

$$B_{0f} = |F_{0f}|^2/|\psi_{3s1/2}(R)|^2 \tag{19}$$

$$B_f = |F_f|^2/|\psi_{3s1/2}(R)|^2 \tag{20}$$

B_{0f} is the correction including only the overlaps between the initial and the final atom, while B_f includes the overlap and exchange corrections. Bahcall [23, 24] was the first to include the overlap and exchange corrections. Faessler et al. [25] included also selfconsistently the effect of holes in the daughter atom on the electron wave functions.
A first orientation is obtained, if one sets the 'diagonal' overlaps $< k'|k >$ of electron orbitals with the same quantum numbers $n,\ \ell,\ j$ in the initial and the final atom equal to unity and the $'non-diagonal'$ overlaps equal to zero. In this approximation $|b >$ is the electron removed from the parent (Holmium). But the state $|b' >$ in the overlap is an electron in the daughter (Dysprosium). $|f' >$ is the hole state in the daughter. But for the overlap $< b'|f >$ in eq. (23) the corresponding electron state in the parent is needed. It seems, that Vatai [26, 27] used the approximation putting all "diagonal" overlaps to unity $< k'|k >= 1.0$ and neglecting the exchange contributions. (Here labeled by "Approx0" and also some times called the Vatai approximation [26, 27], used also by De Rujula in ref. [16].)

$$F_{0f}(Approx0) = \psi_f(R) \tag{21}$$

In the Vatai approximation [26, 27], used also by De Rujula [16], the overlap and exchange correction factor B_f of eq. (3) simplifies.

$$B_{0f}(Approx0) = (\psi_f(R)/\psi_{3s1/2}(R))^2 \tag{22}$$

The subscript f indicated the atomic orbital of the parent, from which the electron is captured. Vatai and De Rujula [16] use this expression at the origin $R\ =\ 0.0$. In a slightly improved version one can also include exchange terms.

$$F_f(Approx) = \psi_f(R) - \sum_{b \neq f} \psi_b(R) < b'|f > \tag{23}$$

$$B_f(Approx) = (F_f(approx)/\psi_{3s1/2}(R))^2 \tag{24}$$

The overlaps listed in table 2 show , that indeed this approximation can give a first quite reasonable approximation. But for all results reported here, if not otherwise stated, we use the exact expressions. The relative plus and minus signs of states, which mix for different n but the same ℓ and j, are essential. But an overall minus sign is irrelevant.

The single electron states occupied in the Holmium ground state are:

$$\begin{gathered}(|1s_{1/2} >)^2, (|2s_{1/2} >)^2, (|2p_{1/2} >)^2,\\ (|2p_{3/2} >)^4, (|3s_{1/2} >)^2, (|3p_{1/2} >)^2,\\ (|3p_{3/2} >)^4, (|3d_{3/2} >)^4, (|3d_{5/2} >)^6,\\ (|4s_{1/2} >)^2, (|4p_{1/2} >)^2, (|4p_{3/2} >)^4,\\ (|4d_{3/2} >)^4, (|4d_{5/2} >)^6, (4f_{5/2} >)^6,\\ (|4f_{7/2} >)^5, (|5s_{1/2} >)^2, (|5p_{1/2} >)^2,\\ (|5p_{3/2} >)^4, (|6s_{1/2} >)^2;\end{gathered} \tag{25}$$

Using like Vatai [27] - but in our case in a relativistic treatment - the approximation as in eq. (21) one get a simple expression for $F_f(approx0)$ used also by De Rujula [16]. The amplitudes F_f and its approximations as described above are given in table 3.

The 163 Dysprosium ground state with $Z\ =\ 66$ has only 4 electrons in $(|4f_{7/2} >)^4$. The small Q-value of electron capture in 163 Holmium to 163 Dysprosium of $Q\ =\ 2.3\ to\ 2.8\ keV$ is optimal for

the determination of the electron neutrino mass. It also restricts the excited hole states in Dysprosium to $3s_{1/2}$ (M_1) and higher. The experimental excitation energies of the hole states and there widths are given in eq.(26) taken from reference [28]. (See also [15, 22, 29].)

$$\begin{aligned} E(3s_{1/2}, M_1) &= 2.040keV;\ \Gamma = 13.7eV; \\ E(3p_{1/2}, M_2) &= \ 1.836keV;\ \Gamma = \ 7.2eV; \\ E(4s_{1/2}, N_1) &= 0.411keV;\ \Gamma = \ 5.3eV; \\ E(4p_{1/2}, N_2) &= 0.333keV;\ \Gamma = \ 8.0eV; \\ E(5s_{1/2}, O_1) &= 0.048keV;\ \Gamma = \ 4.3eV; \end{aligned} \tag{26}$$

For the excited Dy atom with a hole in a singly occupied $(|3s_{1/2}>)^1$ the number of electrons in $|4f_{7/2}>$ is five. As an example lets write down the expression (17) for capture into the final $M1 \equiv 3s$ state .

$$\begin{aligned} F_{3s,Dy} = \psi_{3s,Ho}(R) &< 1s'|1s>^2 \cdot < 2s'|2s>^2 \cdot < 3s'|3s>^1 \\ &\cdot < 4s'|4s>^2 \cdot < 5s'|5s>^2 \cdot < 6s'|6s>^2 \\ &\cdot < 2p'_{1/2}|2p_{1/2}>^2 \cdot < 3p'_{1/2}|3p_{1/2}>^2 \\ &\cdot < 4p'_{1/2}|4p_{1/2}>^2 \cdot < 5p'_{1/2}|5p_{1/2}>^2 \\ &\cdot < 2p'_{3/2}|2p_{3/2}>^4 \cdot < 3p'_{3/2}|3p_{3/2}>^4 \\ &\cdot < 4p'_{3/2}|4p_{3/2}>^4 \cdot < 5p'_{3/2}|5p_{3/2}>^4 \\ &\cdot < 3d'_{3/2}|3d_{3/2}>^4 \cdot < 4d'_{3/2}|4d_{3/2}>^4 \\ &\cdot < 3d'_{5/2}|3d_{5/2}>^6 \cdot < 4d'_{5/2}|4d_{5/2}>^6 \\ &\cdot < 4f'_{5/2}|4f_{5/2}>^6 \cdot < 4f'_{7/2}|4f_{7/2}>^5 \\ - \sum_{b=1\ldots Z \neq 3s} &\psi_{b,Ho}(R) < b'|3s> \prod_{k\neq(3s,b)} < k'|k> \end{aligned} \tag{27}$$

The primed $|k'>$ states are in the daughter (Dysprosium) atom and the unprimed single electron orbits in the parent atom (Holmium) $|k>$. These two orbits with the same $n,\ \ell\ and\ j$ have still a large overlap close to unity (see table 2). The sum over b runs also over b' and is restricted by orthogonality to the $ns_{1/2}$ electrons in Ho excluding the $3s_{1/2}$ level. $|f'>$ are the empty electrons states in the daughter atom (Dysprosium). The wave functions $\psi_b(R) = \psi_{b,Ho}(R)$ have to be taken at the position of the nucleus in the Holmium atom. More exactly they should be integrated over the nucleus with the weak interaction Hamiltonian with the weight r^2. Since the surface of the nucleus has the largest weight for EC the values of $\psi_{b,Ho}(R)$ are taken in this work for the upper spinor component for the $ns_{1/2},\ P_s(R)/R$ and for the lower component $np_{1/2},\ Q_{p1/2}(R)/R$ at the nuclear radius R.

In the selfconsistent Dirac-Fock approach [18, 19, 20] we include the finite size of the nucleus as Fermi distribution with a diffuseness adjusted to electron-nucleus scattering data [30].

$$\rho(r) = \frac{\rho_0}{1 + exp[(r-R)/a]} \tag{28}$$

$$a = 0.546\ [fm] = 1.0318 \cdot 10^{-5}\ [au]; \tag{29}$$

The length for the atomic units $[au]$ is the Bohr radius of Hydrogen.

$$1[au] = 0.529177 \cdot 10^{-8}\ [cm]; \tag{30}$$

The charge parameter of the nucleus ρ_0 is normalized in Holmium to a total charge of $Z = 67$ and in Dysprosium to $Z = 66$ protons in the nucleus. The diffuseness a is taken from the book of Fraufelder

and Henley [30]. The wave function of the captured electron in the parent atom (here Holmium with $Z = 67$ and $A = 163$) should be integrated over the nucleus. In almost all previous calculations of the overlap and exchange contributions for electron capture either a point nucleus is assumed or/and the captured electron wave function is taken at the origin. In this work the nucleus is treated with a finite charge distribution (28) and the value of the captured electron wave function is taken at the nuclear radius. For capture from $s_{1/2}$ states the upper $P_{ns1/2}(R)/R$ and for capture from $p_{1/2}$ states the lower radial spinor waves $Q_{np1/2}(R)/R$ (9) are used. An overall sign in eq. (17) and in eq. (27) is accidental and is also irrelevant, since the expression enters as absolute squared.

Bahcall [23, 24] studied non-relativistically in lighter atoms $Z = 14$ to 37 the overlap and exchange corrections. The non-relativistic treatment restricts to capture of $ns_{1/2}$ electrons. In his case the wave functions of the captured electrons are taken at the origin $\psi_{ns1/2}(0)$ and a point nucleus is assumed. Hole states for the determination of the electron wave functions of the daughter atom and also the multiplicity of several electrons in the same orbit are not included for the overlap and exchange corrections. Faessler et al. [25] were the first to include hole states for the selfconsistent determination of the electron wave functions in the daughter nucleus.

The approximate expressions used by Bahcall [23, 24] for much lighter systems in a non-relativistic treatment are:

$$F_{1s'}(Bahcall) =< 2s'|2s >< 3s'|3s > \psi_{1s1/2}(0)$$
$$- < 2s'|1s >< 3s'|3s > \psi_{2s1/2}(0) - < 3s'|1s >< 2s'|2s > \psi_{3s1/2}(0) \quad (31)$$

$$F_{2s'}(Bahcall) =< 1s'|1s >< 3s'|3s > \psi_{2s1/2}(0)$$
$$- < 1s'|2s >< 3s'|3s > \psi_{1s1/2}(0) - < 3s'|2s >< 1s'|1s > \psi_{3s1/2}(0) \quad (32)$$

Vatai [26, 27] derived using explicitly Slater determinants the non-relativistic equivalent of the formulation given here. We used second quantization. He includes for the overlaps (10) in his theoretical formulation the multiplicity of electrons in the same orbit, but as it seems not in the numerical calculations, where he did set all overlaps of equivalent orbitals $< k'|k > \equiv 1.0$ of the parent $|k >$ and the daughter $|k' >$ equal to unity, so that the multiplicity problem is not relevant for him. (See eqs. (5) and (6) of ref. [27]). The existence of holes in the final atom seems not to be included in the numerical treatment, although the problem is discussed. (See ref. [26] page 542 (ii)). The nucleus seems be treated as point like. (See [26] page 545 chapter 3.1.)

Lets assume one has measured or calculated the electron capture probability $P(n_0,\ \ell_0,\ j_0)$ into the daughter (Dysprosium) state $|n_0, \ell_0,\ j_0 >$, what is then the probability for EC into an other final hole state $P(n,\ \ell,\ j)$?

$$Br(n,\ \ell,\ j/n_0,\ \ell_0,\ j_0) = \frac{P(f = n,\ \ell,\ j)}{P(f_0 = n_0,\ \ell_0,\ j_0)} = \frac{B_{f=n\ \ell\ j} \cdot |\psi_f(R)|^2}{B_{f_0=n_0\ \ell_0\ j_0} \cdot |\psi_{f0}(R)|^2} \quad (33)$$

with B_f from eqs. (12), (17) and (20). These values are listed in table 4.

3 Numerical Results.

The theoretical calorimetric spectrum of the bolometer for the decay of the single hole states in Dysprosium is shown in figure 1 with the relative overlap and exchange corrections $Br(n,\ \ell,\ j/\ n_0,\ \ell_0, j_0)$

eq. (33) given in table 4. By choosing all overlap and exchange correction factors unrealistically in eq. (3) $B_f = Br = 1.0$ the corresponding results a displayed in figure 2. With this choice for the factors $B_f = 1.0$ they disappear from eq. (3). Loosely speaking one can say that this choice yields results "without overlap and exchange corrections". Figure 2 and 6 show such results with this unrealistic choice of all $B_f = 1.0$ as an information for the reader. Figure 3 shows the experimental spectrum according to [31, 32]. A comparison of these three figures shows the need for the "overlap and exchange correction factors" B_f.
To see also the spectrum in between the resonances, which stand out in figures 1 and 2 and also in the experimental spectrum fig. 3, the logarithmic theoretical spectrum for the value $Q = 2.80\ keV$ is shown in figure 4 for the neutrino mass $m_\nu = 0\ eV$ with overlap and exchange corrections.

De Rujula [16] shows also the logarithmic spectrum for the Q-value $Q = 2.5\ keV$ in his figure 12 with older values for the excitation energies of the hole states and their width in Dysprosium. Newer values [28] used here are listed in eq. (26). To estimate the overlap corrections De Rujula used the "Vatai"-approximation, called in the present paper "Approx0" in eqs. (19) and (21) [26] and [27], which assumes a 100 percent overlap between the corresponding electron wave functions in Holmium and in Dysprosium and neglects all exchange corrections. He takes the electron wave functions in Ho at the origin from tables of reference [33]. The correction applied by De Rujula [16] is then simply

$$Br(De\ Rujula; f/3s_{1/2}) = (\psi_f(0)/\psi_{3s1/2}(0))^2 \tag{34}$$

with $\psi_{3s1/2}(0) = \psi_{M1}(0)$ instead of the more exact expression of eq. (33) with (17) and (20). De Rujula takes the wave functions $\psi_f(0)$ and $\psi_{3s1/2}(0)$ at the origin in Holmium for the corresponding quantum numbers $|f> = |n,\ \ell,\ j>$ of the hole states in Dysprosium from ref. [33]. In this work the wave functions are taken at the nuclear radius, since in the nuclear matrix element the electron wave functions are integrated over the whole nucleus with a weight factor r^2. The factor r^2 suppresses the influence of $\psi_f(r)$ at $r = 0$.

Our spectrum at the upper end $< 2.79\ keV,\ 2.80\ keV >$ is given for the neutrino masses $m_\nu = 0,\ 2,\ 5\ eV$ with and without the relative overlap and exchange corrections Br defined in eq. (33) with (20) (numerical values in table 4) in figures 5 and 6. The end point of the theoretical calorimetric spectrum is determined by the Q value and the neutrino mass and thus is the same with and without overlap and exchange corrections. But the slope of the spectrum near the end point is slightly different. Due to the experimental finite energy resolution one cant determine the neutrino mass just by looking to the disappearance of the spectrum. One will need to perform a least square fit to the data of the theoretical spectrum near the end point varying the Q-value, the neutrino mass and probably also the finite energy resolution including also a background. So figure 5 could be the starting point of such a fit.

Table 4 gives the probabilities for the $4s_{1/2}, 5s_{1/2}, 3p_{1/2}, 4p_{1/2}$, and $5p_{1/2}$ holes relative to the 3s hole in Dy with a vacancy in these states. Due to the small $Q \approx 2.5[keV]$ Q-value only $3s, 4s, 5s, 6s$ and $3p_{1/2}, 4p_{1/2}, 5p_{1/2}$ holes can be excited.

In table 5 the relative probabilities also for the excitation of other hole states in ^{163}Dy apart of $s_{1/2}$ and $p_{1/2}$ are given. These other hole states can be excited due to the description of the nucleus with a finite Fermi charge distribution (28), (29) and (30). Electron capture is proportional to the probability to find the electron inside the nucleus weighted with r^2. This emphasizes the role of the electron wave functions at the nuclear radius. There also other than $s_{1/2}$ and $p_{1/2}$ electron wave functions are different from zero. For the determination of the relative probabilities in table 5 the Vatai approximation (34) is used, since this approximation already shows, that capture from other than $s_{1/2}$ and $p_{1/2}$ states can be neglected. The results in table 4 are calculated with the exact expressions (33).

4 Neutrino Mass, Energy Resolution and the Electron Capture Spectrum of ^{163}Holmium.

The experimental bolometer spectrum of EC in ^{163}Ho has a finite energy resolution characterized by the "Full Width Half Maximum (FWHM)". This complicates the extraction of the neutrino mass from the upper end of the bolometer spectrum near the Q value. In figures 7 and 8 the effect of finite energy resolution is shown.

Figure 7 displays for neutrino masses 0 eV and 1 eV the bare theoretical spectra and the two spectra width FWHM (Full Width Half Maximum) = 1 eV. After folding the complete $< 0.000\ [keV]; 2.802\ [keV] >$ bare theoretical spectrum with a Gaussian the integral over the bare and the folded spectrum has the same value. But this is not the case for a finite folding interval, here $< 2.7500\ [keV];\ 2.8020\ [keV] >$. Strength from the left side of the lower bound of the energy of the integral can not be moved into the folding area and strength from the folding interval is moved on the left side outside the integral below 2.75 keV and lost. The effect is for 1 eV FWHM a reduction of the folded spectrum practically independent of the assumed neutrino mass by 1 %. A renormalization of the folded spectrum by multiplying it by a factor 1.01 can practically not been seen in the figure and thus is not shown. In addition such a renormalization factor should depend on the energy.

But if one integrates the spectrum folded in the interval $< 2.7500\ [keV]; 2.8020\ [keV] >$ over a smaller interval $< 2.7500 + N*FWHMkeV;\ 2.820\ keV >$ with $N > 5$ the integral is even slightly larger than the one over the bare spectrum. (Hardly visible in the figure and thus not included in it.) This is due to the rapid decrease of the spectrum with increasing energy at the upper end near the Q value. The folding moves more relative intensity to the right than to the left over the initial energy of the integration. Figure 7 displays the last 80 mesh points for the energy interval $< 2.7947\ [keV]; 2.8020\ [keV] >$ corresponding to 7.3 eV for a spectrum folded over the interval $< 2.7500\ [keV];\ 2.8020\ [keV] >$.

Figure 8 shows the same as figure 7 but for the $FWHM = 3\ eV$ for a Gaussian folded into the spectrum in the interval $< 2.7500\ [keV];\ 2.8020\ [keV] >$. The integral over the folded spectrum is now 3 % smaller than the same integral over the bare spectrum due to the three times larger FWHM of the Gaussian. But it is still so small, that a renormalization of the folded spectrum by a factor 1.03 can hardly be seen in figure 8 and thus is not shown here.

To determine the neutrino mass from EC in ^{163}Ho the electron capture data must probably be adjusted with a maximum likelihood method varying the neutrino mass, the Q-value and probably also the energy resolution to simulations like in figures 7 and 8, since not only the neutrino mass, but also the Q value and the energy resolution are not known accurately enough. The overlap and exchange corrections affect the slope of the spectrum just below the Q value, thus these corrections must be included in such an analysis.

5 Technical Details.

Figures 9 and 10 show the connection between the 251 logarithmic arranged radial mesh points t and the radius in atomic units $[au = a_0 = Bohr\ radius = 0.529177 \cdot 10^{-8}[cm]]$. Figure 11 shows the upper amplitudes $P_{ns1/2}$ (9) for $n = 1, 2, ...6$ in Holmium as a function of the radial parameter t eqs. (35), (36) and (37).

$$t = \ln(r/r_0)/h;\quad h = 0.05;\quad r_0 = 7.1469 \cdot 10^{-5}[au].\ \ t = 1, 2, ...251 \tag{35}$$

Figure 12 demonstrates, that at small radial distances from the origin the lower component $Q(r)$ for $2p_{1/2}$ is larger than the upper component P(r). Figure 13 shows the amplitudes $P(r)/r$ and $Q(r)/r$ (9)

for $1s_{1/2}$ and $2p_{1/2}$ and hints , that the lower component $Q_{2p1/2}(r)/r$ approaches a value different from zero at the origin.

Table 1 shows the relativistic wave functions $P_{ns}(R)/R$ and $Q_{ns}(R)/R$ and also $P_{np1/2}(R)/R$ and $Q_{np1/2}(R)/R$ at the nuclear radius calculated and used in this work. These values are compared with the non-relativistic Froese-Fischer (FF) [34] and the relativistic results of Mann and Waber (MW) [35] at the origin for the upper (u) and the lower (ℓ) amplitude (9). At $r = 0$ the lower $ns_{1/2}$ and the upper $np_{1/2}$ components (9) are zero.

Table 2 lists the overlaps $< n', s'_{1/2}|n, s_{1/2} >$ and $< n', p'_{1/2}|n, p_{1/2} >$ of $A = 163$ Dysprosium states $< k'|$ with a hole in $3s'$ (M'_1) with states $|k >$ in the parent Holmium. Table 3 gives the amplitudes (21), (23), (16) and (17) calculated with our relativistic values $\psi(R)$ and overlaps and also the corresponding results with the relativistic wave functions $\psi(0)$ tabulated by Mann and Waber [35] at the origin and our overlaps (see for example table 2).

To calculate the electron capture correction factors B_f (3) [23, 24, 25, 26, 27] for $^{163}_{67}Ho \rightarrow ^{163}_{66}Dy$ in eqs. (3), (12) and (20) one assumes, that the two ground states and the states of Dy with electron vacancies in the different states $1s_{1/2}$ (K), $2s_{1/2}$ (L_1), $3s_{1/2}$ (M_1), $4s_{1/2}(N_1)$ *and* $5s_{1/2}$ (O_1) and also $2p_{1/2}$ (L_2), $3p_{1/2}$ (M_2), $4p_{1/2}$ (N_2) *and* $5p_{1/2}$ (O_2) can be described by a selfconsistent Slater determinant. We use here selfconsistent relativistic wave functions for the ground states in Holmium and in Dysprosium and allow also explicitly electron vacancies in the specific final hole states using the Dirac-Fock code of Grant [18] with modifications and simplifications by Desclaux [19] and Ankudinov et al. [20]. Relativistic effects contract the inner electron shells and increase in Z = 67 nuclei the amplitudes of the electrons at the nucleus $\psi_{b,Ho}(0)$ by about a factor 2. In addition apart of the $\ell = 0$ states also the $p_{1/2}$ states have, due to the lower (so called 'small') amplitude, a finite probability to be at the nucleus. The correction factor $B_{n\ell\ j,Dy}$ depends only on the relative size of $\psi_{n\ell\ j,Dy}(R)/\psi_{n0,\ell 0,\ j0,Dy}(R)$. The $\psi_{n\ p1/2}(R)$ amplitudes of $n\ p1/2$ are 0.20 to 0.25 of the corresponding $|n,\ s_{1/2} >$ states or 4 to 5% for the probability relative to the s states. But care has to be taken, since in the interference terms the corrections are proportional to the amplitudes. In Holmium and Dysprosium a relativistic treatment is definitely needed. (See also reference [36].)

For the ground state of Holmium the electron multiplicities the occupation of the different orbitals are given in eq. (25). The occupation of the ground state and the excited hole states of Dysprosium are discussed after eq. (25). The occupation of the in the ground states of $4f_{7/2}$ is 5/8 in Ho and 4/8 in Dy.

The scale t is logarithmic in the radial distance. The relation between the radius and the distance parameter t is shown in figures 9 and 10. The choice of t in figures 11, 12 and 13 displays more in detail the area around the nucleus, where the potential is changing fast. The 251 mesh points are defined as $t = 1, 2, ...251$ [20]:

$$r = r_0 e^{ht}\ [au]\ ;\quad t\ =\ 1,\ 2, ...\ 251 \tag{36}$$

$$r_0 = 7.14693 \cdot 10^{-5}\ [au];\quad ; h = 0.05\quad for\quad Holmium \tag{37}$$

$$r_0 = 14.33817 \cdot 10^{-5}\ [au];\quad ; h = 0.05\quad for\quad Dysprosium \tag{38}$$

To guarantee the accuracy needed [20] we use double precision. To obtain the wave functions at the same meshpoints for Ho and for Dy we use fourth order Lagrange interpolation. The integrations are performed with Simpson. The logarithmic radial scale $t\ =\ 1, 2, ...251$ for the figures is always translated to the convention for Holmium (37).

6 Conclusion

The main aim of this work is to study the effect of a finite electron neutrino mass on the calorimetric spectrum of the deexcitation of the hole states in ^{163}Dy after electron capture in ^{163}Ho. A finite neutrino mass suppresses counts in the spectrum around the interval $(Q - m_\nu, Q)$. Since one does not know the Q value exactly and since the energy resolution is not perfect, one needs to know the theoretical calorimetric spectrum for extracting the neutrino mass as a function of the neutrino mass, the Q value and probably also of the energy resolution. This is similar as for the determination of the anti-neutrino mass in the Tritium decay of the KATRIN experiment. The theoretical figures 1 and 2 and the experimental spectrum in fig. 3 [31] show, that the relative overlap and exchange corrections of eq. (33) are very essential for the form of the spectrum (3). From the results presented it is also clear, that only a fully relativistic selfconsistent treatment can be reliable. The "small" parameter $Z/137 = 0.49$ for a non-relativistic approach is not so small and relativistic effects must be included. They contract the inner electron shells and increase the electron wave functions at the Holmium nucleus by about a factor 2 (see table 1), which increases the absolute value of the capture cross section by a factor four. The relative difference between Z for the parent and $(Z-1)$ for the daughter is getting smaller for heavier atoms. Thus the effect of the overlap and exchange corrections on the absolute value of the capture probability is small. But they regulate the relative weights of the peaks for the different hole states. Thus they have a large effect on the form of the spectrum. The finite energy resolution modifies the bolometer spectrum near the Q value and has to be included extracting the neutrino mass.

Acknowledgment: We want to thank members of the ECHo collaboration for discussions about the ECHo experiment (electron capture in Holmium 163).

References

[1] E. W. Otten, C. Weinheimer, Rep. Prog. Phys. 71 (2008) 086201.

[2] V. M. Lobashev et al., Phys. Lett. B460 (1999) 227.

[3] Amand Faessler, R. Hodak, S. Kovalenko, F. Simkovic, arXiv 1304.5032v3 and "European Physical Journal Web of Conferences".

[4] G. Drexlin, V. Hannen, S. Mertens, C. Weinheimer, arXiv 1307.0101v1.

[5] Carla Macolino, Mod. Phys. Lett. A29 (2014) 1430001.

[6] Dong-Liang Fang, A. Faessler, V. Rodin, F. Simkovic, Phys. Rev. C82 (2011) 0034320 and C83, (2011), 034320.

[7] F. Simkovic, V. Rodin, A. Faessler, P. Vogel, Phys. Rev. C87 (2013) 045501.

[8] L. Gastaldo, K. Blaum, A. Doerr, Ch. E. Duellmann, K. Eberhardt, S. Eliseev, C. Enss, Amand Faessler, A. Fleischmann, S. Kempf et al., arXiv 1309.5214.

[9] L.Gastaldo, P. C. Ranitzsch, F. von Seggern, J. P. Porst, S. Schäfer, C. Pies, S. Kempf, T. Wolf, A. Fleischmann, C. Enss, A. Herlert, K.Johnston, Nuclear Instruments and Methods in Physics Research A711 (2013) 150.

[10] K. Blaum, A. Doerr, C. E. Duellmann, K. Eberhardt, S. Eliseev, C. Enss, A. Faessler, A. Fleischmann, L. Gastaldo, S. Kempf, M. Krivoruchenko, S. Lahiri, M. Matai, Yu. N. Novikov, P. C. Ranitzsch, F. Simkovic, Z. Scusc, M. Wegner, arXiv 1306.2655v1.

[11] Dong-Liang Fang, K. Blaum, S. Eliseev, Amand Faessler, M. I. Krivoruchenko, V. Rodin, F. Simkovic, *Phys. Rev.* C 85 (2012) 054314 .

[12] J. U. Anderson et al. , Phys. Lett. B398 (1982) 72.

[13] F. Gatti et al. , Phys. Lett. B398(1997) 415.

[14] M. I. Kribvoruchenko, F. Simkovic, Dieter Frekers, Amand Faessler, Nucl. Phys. A859 (2011) 140.

[15] M. Wang, G. Audi, et al. Chinese Phys. C **36**, (2012) 1603 and Nuclear Data Tables 35 (1986) 1-13.

[16] A. De Rujula, arXiv 1305.4857v1 [hep-ph] 21 May 2013. A. De Rujula, M. Lusignoli, Phys. Lett. **118 B**, (1982) 429.

[17] W. Bambynek, H. Behrens, M. H. Chen, B. Crasemann, M. L. Fitzpatrick, K. W. D. Ledingham, H. Genz, M. Mutterer, R. L. Intemann, Rev. Mod. Phys. 49 (1977) 109.

[18] I. P. Grant, Adv. Phys. 19 (1970)747.

[19] J. P. Desclaux, Com. Phys. Com. 9 (1975) 31 -45.

[20] A. L. Ankudinov, S. I. Zabinsky, J. J. Rehr, Comp. Phys. Com. 98(1996) 359 -364

[21] G. C. Wick, Phys. Rev. 80 (1950) 268.

[22] P. C.-O. Ranitzsch, J. P. Porst, S. Kempf, et al. Jour. of Low Temp. Phys. 167 (2012)1004 and private communication.

[23] J. N. Bahcall, Phys. Rev.132 (1963), 362.

[24] J. N. Bahcall, Nucl. Phys. 71 (1965) 267.

[25] A. Faessler, E. Huster, O. Kraft, F. Krahn, Z. Phys. 238 (1970) 352.

[26] E. Vatai, Nucl. Phys. A156(1970) 541.

[27] E. Vatai, Nucl. Phys. A402 (1983) 1.

[28] L. Gastaldo, talk at the Heraeus Seminar in Bad Honnef, April 22 - 25 (2014).

[29] G. Audi, A. H. Wapstra, C. Thibault, Nucl. Phys. A279 (2003) 337.

[30] H. Frauenfelder ,E. M. Henley, Subatomic Physics; published by World Scientitific 2007.

[31] L. Gastaldo, K. Blaum, A. Doerr, Ch. E. Duellmann, K. Eberhardt, S. Eliseev, C. Enss, A. Faessler, A. Fleischmann, S. Kempf, P. C.-O. L. Ranitzsch et al., arXiv 1309.5214 [physics.ins-det].

[32] L. Gastaldo et al., Journal of Low Energy Temperature Physics, 176 (2014) 876 - 884.

[33] I. M. Band, M. B. Trhaskovskaya, Atomic Data and Nuclear Data Tables 35, I-13 (1986).

[34] Ch. Froese-Fischer Comp. Phys. Com. 43 (1973) 355.

[35] J. B. Mann, J. T. Waber, Atomic Data 5 (1973) 201.

[36] T. Mukoyama, Bull. Inst. Chem. Rev., Kyoto University, 65 (1987) 17.

Table 1: Electron wave functions of the atomic Holmium ground state at the nuclear radius $R = 6.5551[fm] = 1.238728{\cdot}10^{-4}\,[au]$; $\psi_{b,Ho}(R)\,[au^{-3/2}]$ for the upper (u) $P(R)/R$ and the lower (ℓ) $Q(R)/R$ spinor components of the present relativistic calculations with the Dirac-Fock code of Ankudinov et al. [20] labeled by 'here'. The non-relativistic results (FF) calculated with the Froese-Fischer code [34] are shown at the origin. Non-relativistically the p-waves disappear at $r = 0.0$. The relativistic wave functions of Mann and Waber [35] at the origin $\psi(0)$ for the upper spinor components of the $ns_{1/2}$ (MW u) and for the lower components for the $np_{1/2}$(MW ℓ) wave functions are also listed. The lower spinor component for $ns_{1/2}$ and the upper component for $np_{1/2}$ are zero at the origin. The increase of the wave functions from the non-relativistic to the relativistic approach at the Holmium nucleus at the nuclear radius and at the origin for the upper components of the $ns_{1/2}$ states in the relativistic approach by about a factor 2 is due to relativistic contractions. The phase conventions for our electron wave functions are different compared to the one of Mann and Waber [35].

Holmium	Here u	Here ℓ	FF	MW u	n p1/2	Here u	Here ℓ	MW ℓ
1s	1769	425	1088	2080	2p1/2	37	141	-168
2s	-648	157	359	763	3p1/2	-18	70	-82
3s	303	73	167	357	4p1/2	8.8	33	-39
4s	-146	35	80	172	5p1/2	-3.1	11.6	-13
5s	56	14	30	66	-	-	-	-
6s	-13	3.4	7.3	13	-	-	-	-

Table 2: Overlaps (contractions of Wick's theorem) of the relativistic single electron wave functions of the excited Z = 66 Dysprosium* with a vacancy in the 3s state and Z = 67 Holmium in the ground state for $ns_{1/2}$, $np_{1/2}$ and $np_{3/2}$ for $< n'\ell', Dy(3s)^{-1}|n\ell, Ho >$.

3s Dy hole	1s	2s	3s	4s	5s	6s	-	-
1s'	0.999910	0.008148	-0.003119	0.001433	-0.000546	0.000135	-	-
2s'	-0.007968	0.999716	0.015560	-0.005604	0.002047	-0.000503	-	-
3s'	0.003085	-0.015116	0.999389	0.023618	-0.006894	0.001342	-	-
4s'	-0.001447	0.005660	-0.023007	0.999332	0.013934	-0.003089	-	-
5s'	0.000547	-0.002058	0.006868	-0.013227	0.999510	0.010002	-	-
6s'	-0.000135	0.000506	-0.001653	0.002964	-0.009576	0.999783	-	-
-	$2p_{1/2}$	$3p_{1/2}$	$4p_{1/2}$	$5p_{1/2}$	$2p_{3/2}$	$3p3/2$	$4p_{3/2}$	$5p_{3/2}$
$2p'_{1/2}$	0.999801	0.014854	-0.005069	0.001685	-	-	-	-
$3p'_{1/2}$	-0.013756	0.999563	0.016686	-0.004762	-	-	-	-
$4p'_{1/2}$	0.005058	-0.016148	0.999524	0.011956	-	-	-	-
$5p'_{1/2}$	-0.001671	0.004639	-0.011410	0.999594	-	-	-	-
$2p'_{3/2}$	-	-	-	-	0.999846	0.012517	-0.004483	0.001435
$3p'_{3/2}$	-	-	-	-	-0.012259	0.999648	0.014995	-0.004144
$4p'_{3/2}$	-	-	-	-	0.004481	-0.014573	0.999625	0.010227
$5p'_{3/2}$	-	-	-	-	-0.001428	0.004052	-0.009814	0.999707

Table 3: The first column gives the empty electron states in the daughter atom (Dysprosium). The approximate amplitudes AF_0 (21) and AF (23) and also AFM_0 and AFM [35] are calculated assuming, that the overlaps $< k'|k > = 1.0$ with the same quantum numbers in the parent and the daughter are unity (Vatai approximation [26, 27]). The amplitudes F_0 in eq. (16) and FM_0, include the full overlap corrections but no exchange terms. In this approximation the results in the column AF_0 are given by the upper amplitude (9) as $P(R)/R$ at the nuclear radius for the s-states and by the lower amplitude as $Q(R)/R$ for the $p_{1/2}$-states (see table 1). F_0 includes the overlap corrections. Thus F_0 is always in its absolute value smaller than AF_0. The exchange contributions are then in addition included in F eq. (17) and in FM. All quantities with M are calculated with the tabulated relativistic electron wave functions $ns_{1/2}$ and $np_{1/2}$ of Mann and Waber [35] at the origin $\psi(0)$ with overlaps of this work with relativistic wave functions of the Ankudinov code [20]. (See table 1). The relative sign of wave functions, which mix (same ℓ and j but different n) are important. But a common minus sign of wave function amplitudes is irrelevant, even if they mix. To be consistent in the sign choice between our overlaps and the wave functions of Mann and Waber [35] one has to adjust the phase conventions to each other.

-	AF_0	AF	F_0	F	AFM_0	AFM	FM_0	FM
$1s$	1769.2	1762.7	1767.8	1761.3	2080	2072	2078	2071
$2s$	-648.6	-657.4	-645.1	-653.8	-763	-773	-759	-769
$3s$	303.2	315.1	298.2	309.9	357	371	351	365
$4s$	-146.3	-157.4	-142.4	-153.2	-172	-185	-168	-180
$5s$	56.3	63.3	53.3	55.5	66.3	74.6	62.7	65.3
$2p_{1/2}$	141.6	140.3	140.9	139.7	166.2	167.3	165.4	166.5
$3p_{1/2}$	-69.8	-71.0	-68.7	-69.9	-82	-80	-80	-79
$4p_{1/2}$	33.2	35.1	32.3	34.2	38.9	38.3	37.8	37.3
$5p_{1/2}$	-11.6	-13.0	-11.0	-12.3	-13.6	-12.9	-12.8	-12.2

Table 4: Relative probabilities (33) of capture from $Z = 67$, $A = 163$ Holmium to different states in $Z = 66$, $A = 163$ Dysprosium. Due to the small Q value of around 2.5 keV only vacancies in $M_1(3s_{1/2})$ and $M_2(3p_{1/2})$ and higher can be excited due to energy conservation. (See also (26)). The ratios are $N_1/M_1, O_1/M_1, M_2/M_1, N_2/M_1$ and O_2/M_1. ABr_0 is the approximate expression without exchange terms calculated with AF_0 (21) and ABr with the approximate expression AF (23). The ratios Br_0 and Br are the full expression without exchange and with exchange terms according to eqs. (16) and (17) for the ratios given above. The quantities with M give the equivalent results using the relativistic wave functions at the origin tabulated by Mann and Waber and given in table (1) [35] and the overlaps calculated with our relativistic electron wave functions. (See for example table 2.)
The B_f shown here in column 5 should be used in eq. (3) to calculate the (calometric) bolometer spectrum in arbitrary units to compare with the data of figure 3.

-	ABr_0	ABr	Br_0	Br	ABr_0M	$ABrM$	Br_0M	BrM
$4s$	0.233	0.250	0.228	0.244	0.233	0.249	0.228	0.244
$5s$	0.034	0.040	0.032	0.032	0.034	0.038	0.032	0.032
$3p_{1/2}$	0.053	0.051	0.053	0.051	0.052	0.046	0.052	0.047
$4p_{1/2}$	0.012	0.012	0.012	0.012	0.012	0.011	0.012	0.010
$5p_{1/2}$	0.001	0.002	0.001	0.002	0.001	0.001	0.0013	0.001

Table 5: The relative intensity of electron capture from different orbitals in Holmium relative to capture from the $3s_{1/2}$, M_1 orbit . The finite radius of the nucleus allows also to include capture from other than $ns_{1/2}$ and $np_{1/2}$ electrons. At the radius also other orbitals have wave functions different from zero. The relative intensities are calculated in the so called Vatai [26, 27] approximation (34). The first column gives the quantum number of the denominator, which is always the M_1 orbit $3s_{1/2}$. The quantum numbers in the rows characterize the wave functions for the numerators (34), for which the relative intensity is given. The "ℓ" indicates, that for the $j = \ell - 1/2$ states the larger lower component of the Dirac wave function is used at the nuclear radius. Capture from other than $s_{1/2}$ and $p_{1/2}$ states are extremely small and can be neglected.

-	$3s_{1/2}$	$3p_{1/2}\ell$	$3p_{3/2}$	$3d_{3/2}\ell$	$3d_{5/2}$
$3s_{1/2}$	1.000	0.048	$3 \cdot 10^{-6}$	$2 \cdot 10^{-8}$	$5 \cdot 10^{-13}$
-	$4s_{1/2}$	$4p_{1/2}\ell$	$4p_{3/2}$	$4d_{3/2}\ell$	$4d_{5/2}$
$3s_{1/2}$	0.233	0.012	$7 \cdot 10^{-8}$	$4 \cdot 10^{-9}$	$1 \cdot 10^{-13}$
-	$4f_{5/2}\ell$	$4f_{7/2}$	$5s_{1/2}$	$5p_{1/2}\ell$	$5p_{3/2}$
$3s_{1/2}$	$4 \cdot 10^{-17}$	$7 \cdot 10^{-22}$	0.034	0.002	$8 \cdot 10^{-8}$

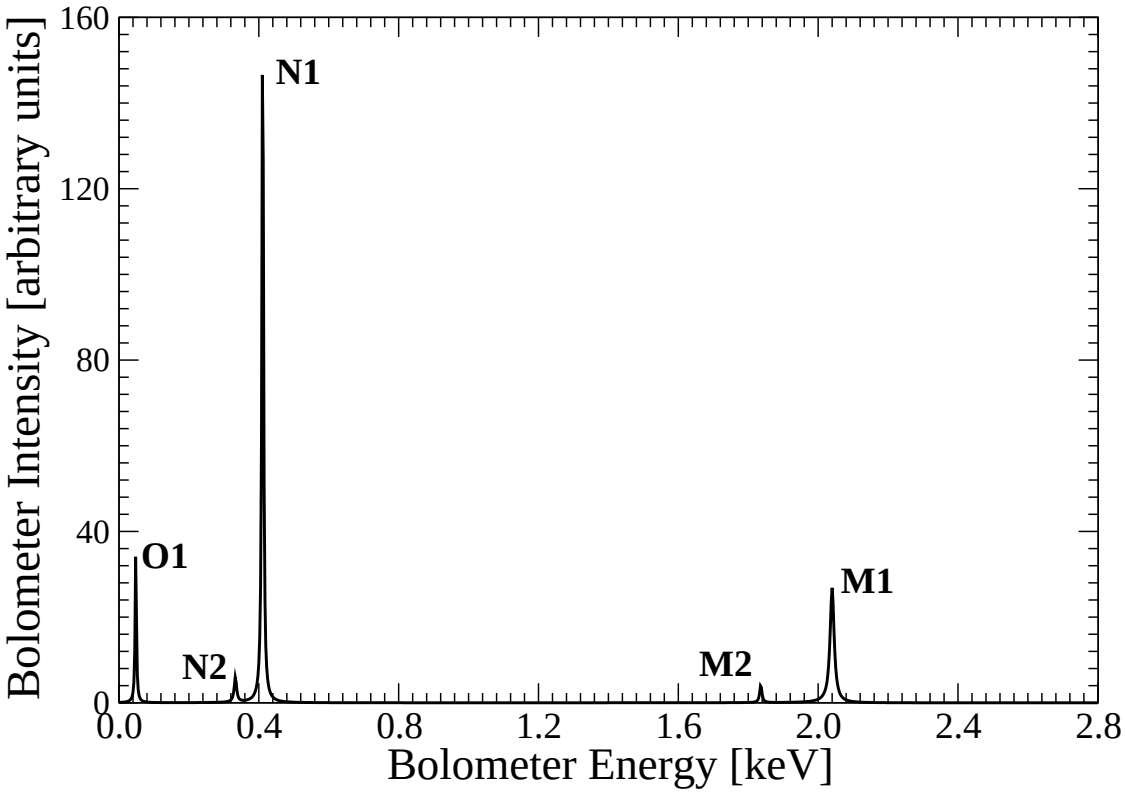

Figure 1: The theoretical bolometer (calorimetric) spectrum of this work of the deexitation of the hole states in Dysprosium in the second step after the initial electron capture in Holmium. The deexcitation energy in the first step is carried away by the neutrino and is not measured. The bolometer sums up all energies emitted in the second step: X-rays, Auger electrons and the recoil of the Holmium nucleus. Since the recoil is in the order of meV, it can be neglected. The spectrum is based on eq. (3) assuming an incoherent deexcitation of the different hole states using experimental energies and width (26). The overlap and exchange correction B_f is included according to to column 5 Br of table 4. The Q value 2.8 keV and the hole binding energies and width eq. (26) are taken from [28]. This spectrum compares well with the data from figure 3. In the mean time the O1 resonance line has also been measured [28]in good agreement with this theoretical results . But since these experimental data are not yet published, it is not shown in figure 3.

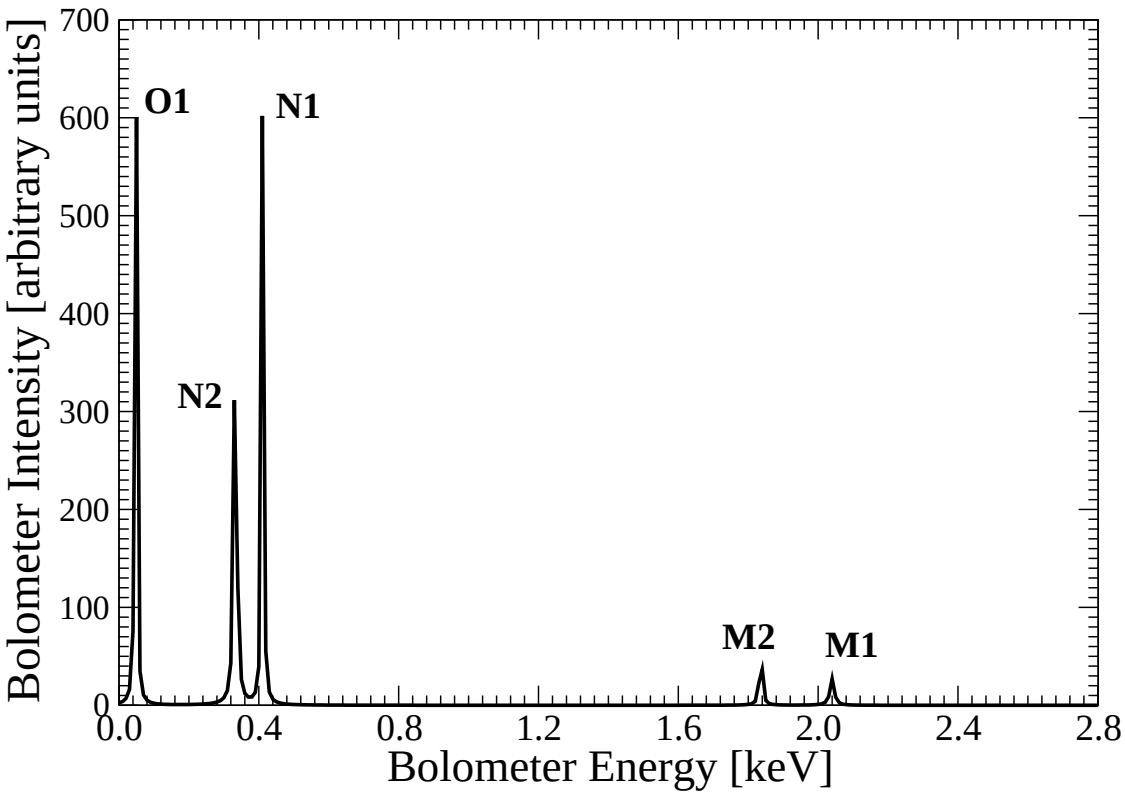

Figure 2: Theoretical spectrum as in figure 1 but with the choice $B_f = B_r = 1.0$ for the capture from all energetically allowed electron levels in 163 $Holmium$. By this unrealistic choice the overlap and exchange coefficients do not show up anymore in eq. (3). Thus one could loosely speaking say the results are calculated "without overlap and exchange correction" B_f. This unrealistic choice of B_f "without overlap and exhange corrections" cant reproduce the data from figure 3.

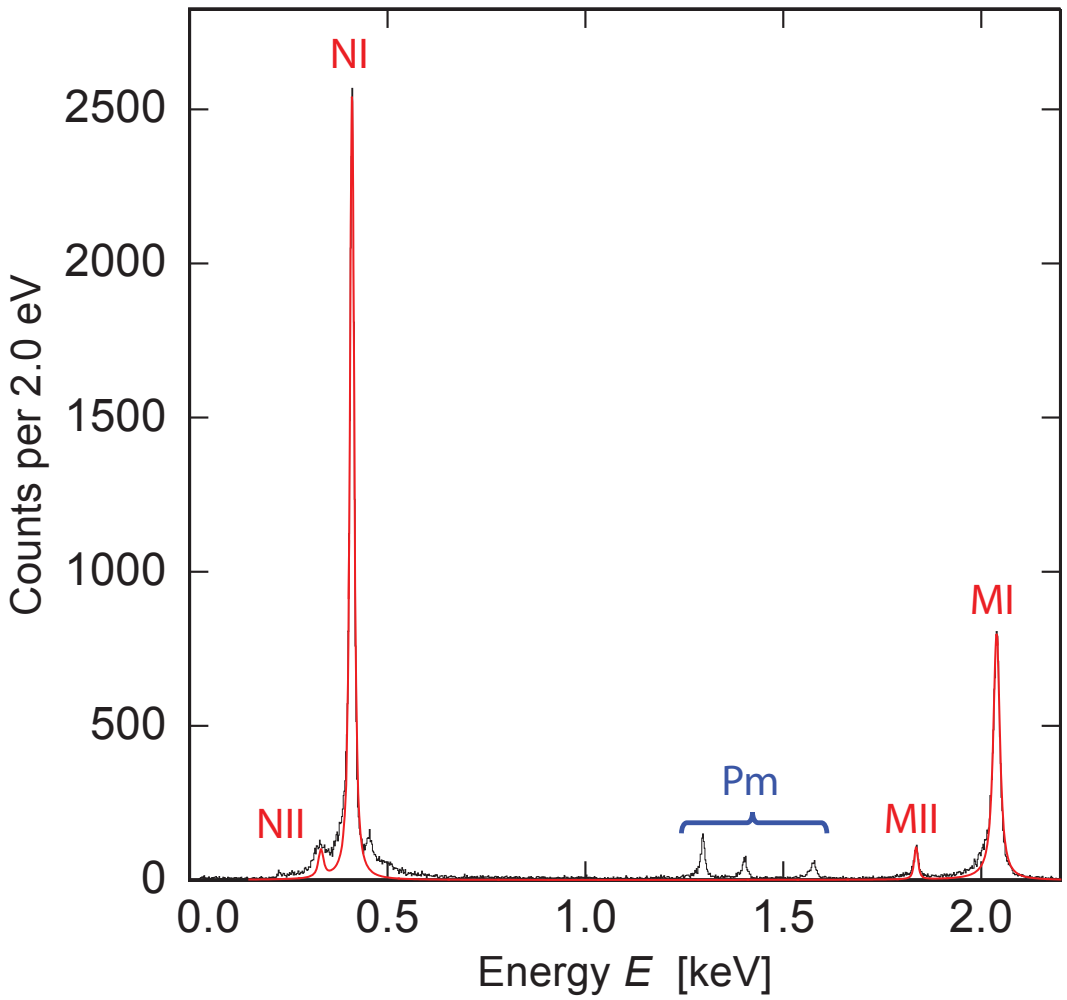

Figure 3: Experimental bolometer (calorimetric) spectrum of the deexitation of the hole states in Dysprosium in the second step after the initial electron capture in Holmium according to [31].

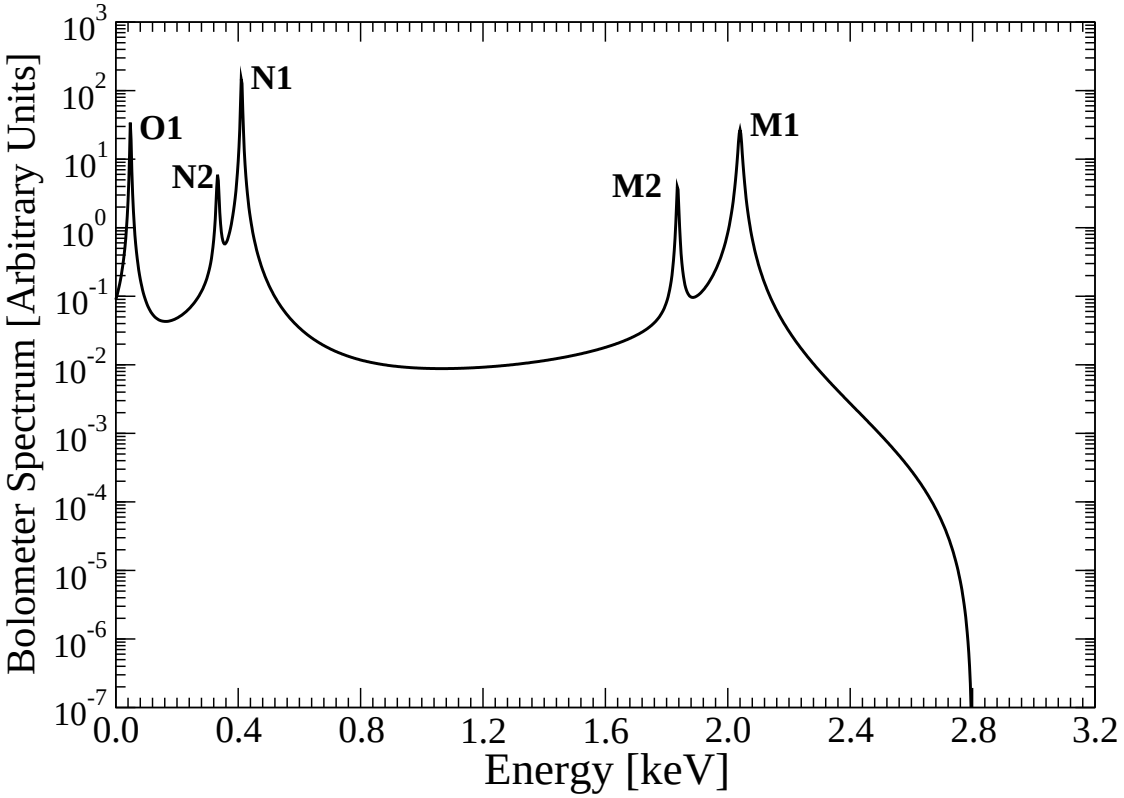

Figure 4: Theoretical logarithmic bolometer (calorimetric) spectrum of the deexitation of the hole states in Dysprosium in the second step after the initial electron capture in Holmium for the Q value 2.8 keV and the neutrino mass $m_\nu = 0.0\ eV$. The overlap and exchange corrections B_f of eq. (3) and eq. (20) from table 4 are included. At this scale of the energy resolution it is not possible to show the theoretical effect of a finite neutrino mass of the order of 1 eV. For the effect of a finite neutrino mass see figure 5.

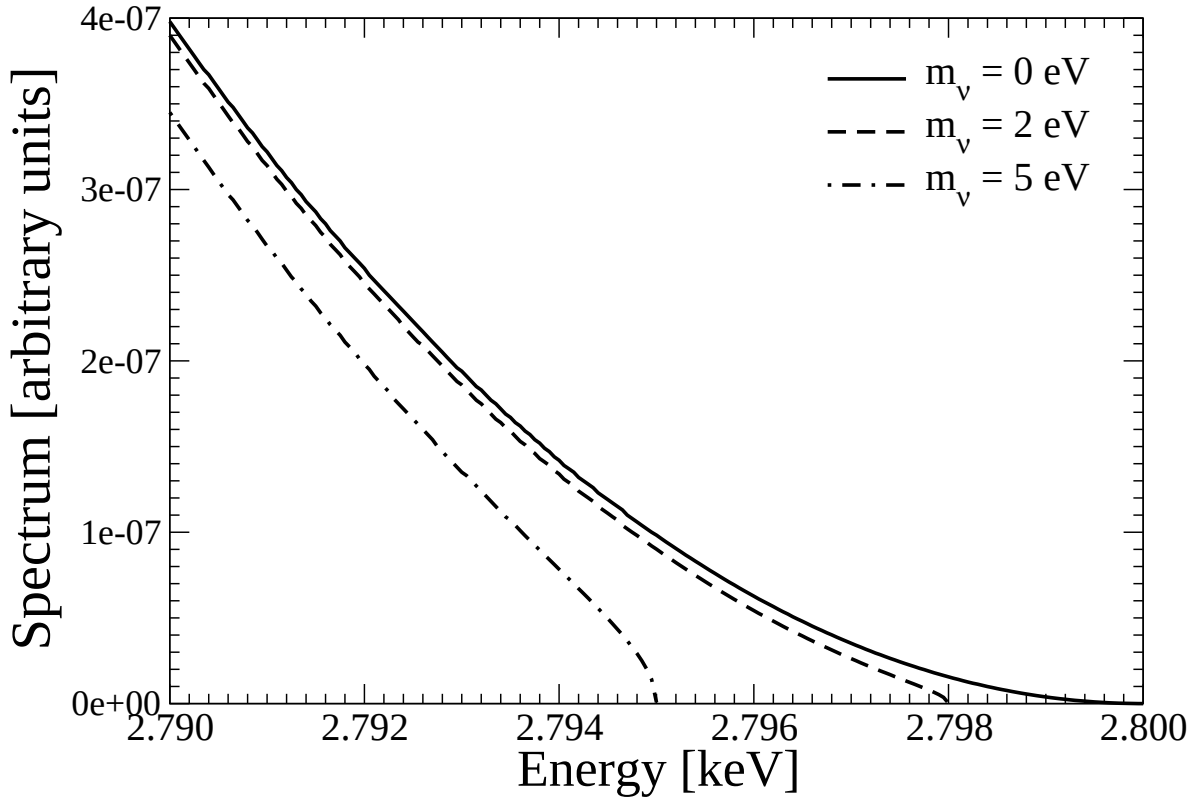

Figure 5: The upper end of the bolometer (calometric) spectrum in the energy interval $2.79\ to\ 2.80keV$ for the deexitation of the hole states in Dysprosium is shown for the neutrino masses $m_\nu\ =\ 0.0\ eV;\ 2.0\ eV\ and\ 5.0\ eV$ and the Q value $Q\ =\ 2.80\ keV$ with the overlap and exchange corrections B_f of eq. (3) included using the values listed in table 4.

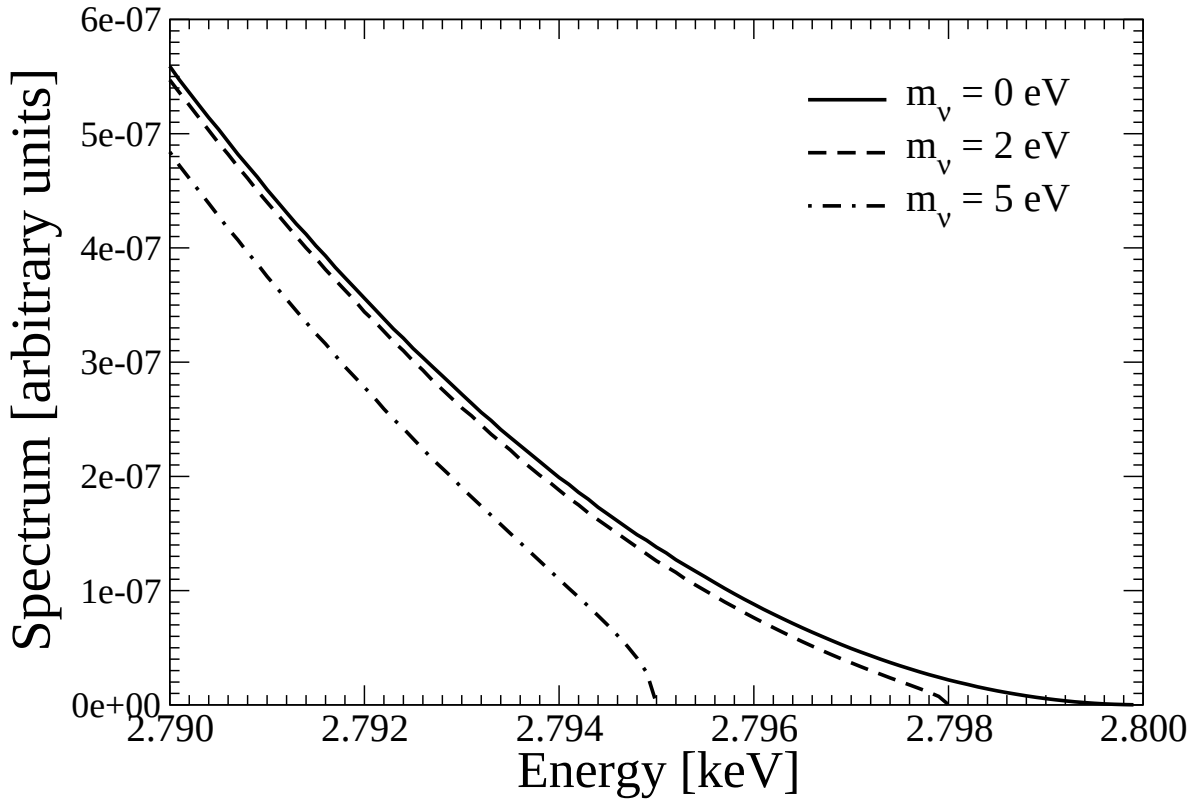

Figure 6: The same bolometer (calorimetric) spectrum as in figure 5 of the deexitation of the hole states in Dysprosium with the unrealistic choice of all overlap and exchange correction factors $B_f = 1.0$. Since then the expressions B_f do then not show up in eq. (3) one can loosely speak of results "without overlap and exchange corrections".

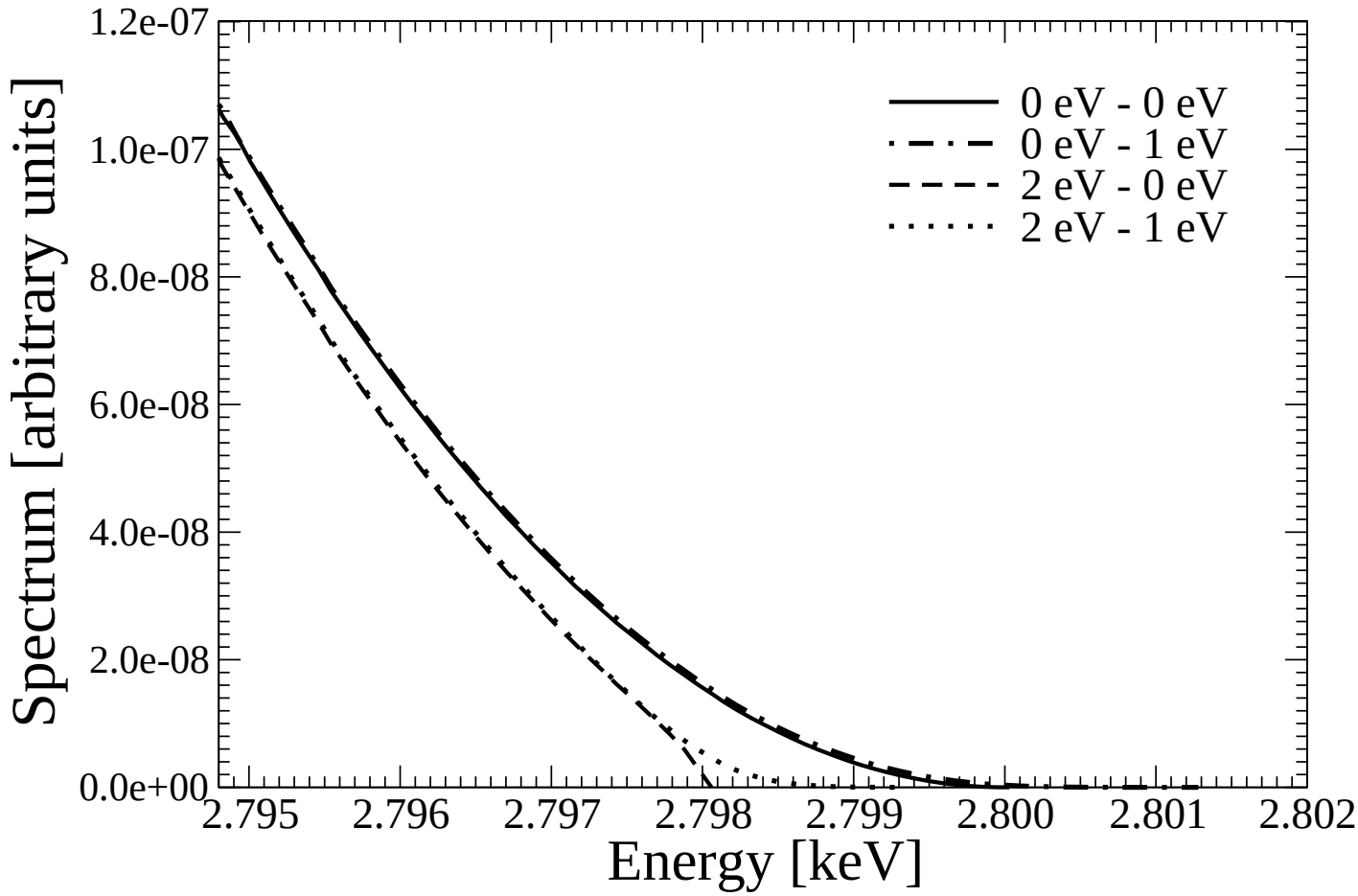

Figure 7: The upper end of the bolometer (calorimetric) spectrum (3) in the energy interval 2.7939 *to* 2.802keV for electron capture in 163 Holmium to 163 Dysprosium for a neutrino mass of 0.0 eV and 2.0 eV with an energy resolution Full Width Half Maximum (FWHM) of 0 eV and 1 eV . (Compare for the same neutrino masses, but different energy resolutions solid with dashed-dotted for $m_\nu = 0.0\ eV$ and dashed with dotted for $m_\nu = 2.0\ eV$.) The Q value is assumed to be $Q = 2.80\ keV$. Folding of the whole spectrum with a Gaussian to include the finite energy resolution of 1 eV FWHM conserves the value of the integral over the whole spectrum. This is not the case, if the folding interval is not the full spectrum. Here the folding is done over 520 mesh points in the interval 2.7500 keV to 2.8020 keV over 52 eV. Energy points below 2.7500 keV do not move strength into the folding interval and energy points just above or equal 2.7500 keV move strength down below 2.7500 keV and this strength is lost for the folded spectrum. The integral over the folded spectrum above 2.7500 keV is slightly by about 1 % (independent of the neutrino mass by about a factor 0.991) smaller than the integral over the bare theoretical spectrum. This difference cant be seen in a figure and thus a renormalized curve is not shown. The overlap and exchange corrections B_f of eq. (3) are included according to table 4. The calculations are performed with double precision to obtain the required accuracy.

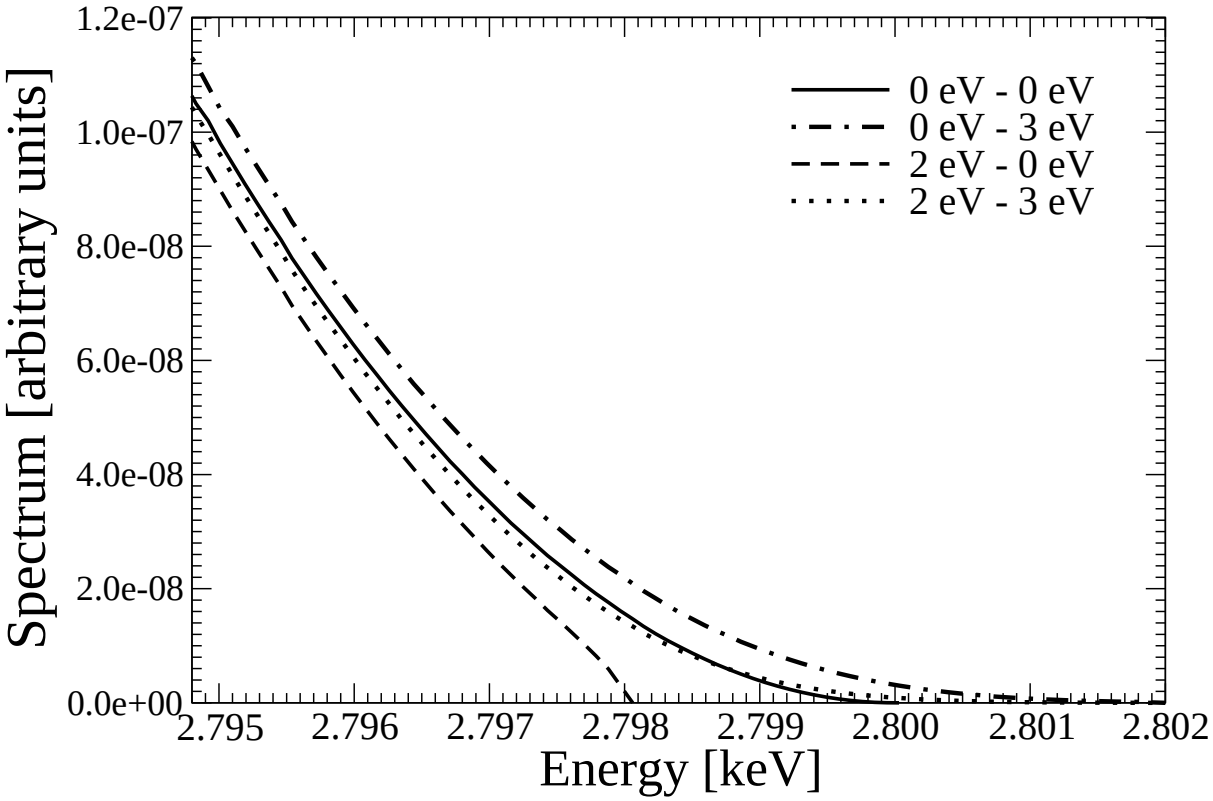

Figure 8: The upper end of the bolometer (calorimetric) spectrum of electron capture in 163 Holmium to 163 Dysprosium (3) for a neutrino mass of 0.0 and 2.0 eV, with an energy resolution $FWHM = 0.0\ eV$ and $3.0\ eV$. (Compare for the same neutrino masses and for different energy resolutions solid with dashed dotted for $m_\nu = 0.0\ eV$ and dashed with dotted for $m_\nu = 2.0\ eV$.) The integral over the spectrum $< 2.75\ [keV;\ 2.802\ [keV] >$ folded with a Gaussian with the Full Width Half Maximum (FWHM) of $3\ eV$ is slightly by about 3 % smaller. The reasons are explained in figure 7. The exact reduction factor is by a factor three larger than for the folded spectrum with 1 eV FWHM from figure 7, where the reduction is only 1 %. The assumed Q value is $Q = 2.80\ keV$. The overlap and exchange corrections B_f of eq. (3) are included according to table 4. More details in the caption of figure 7.

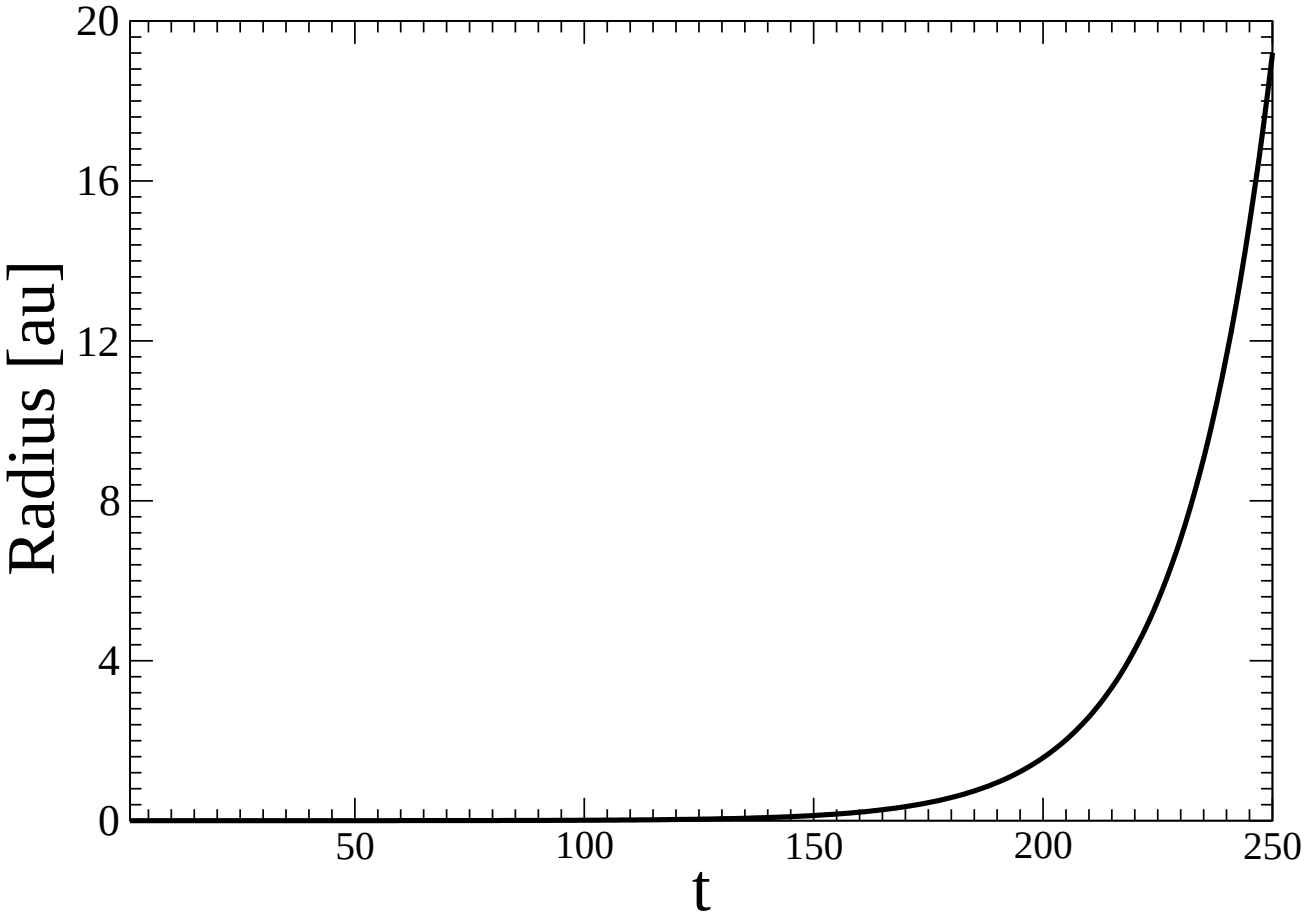

Figure 9: Radial distance in a logarithmic scale $t = ln(r/r_0)/0.05$, where t counts the radial meshpoints $t = 1$ *to* 251. r in atomic units (Bohr radii $[a_0]$) for Holmium with $r_0 = 7.14693 \cdot 10^{-5}$ $[au]$.

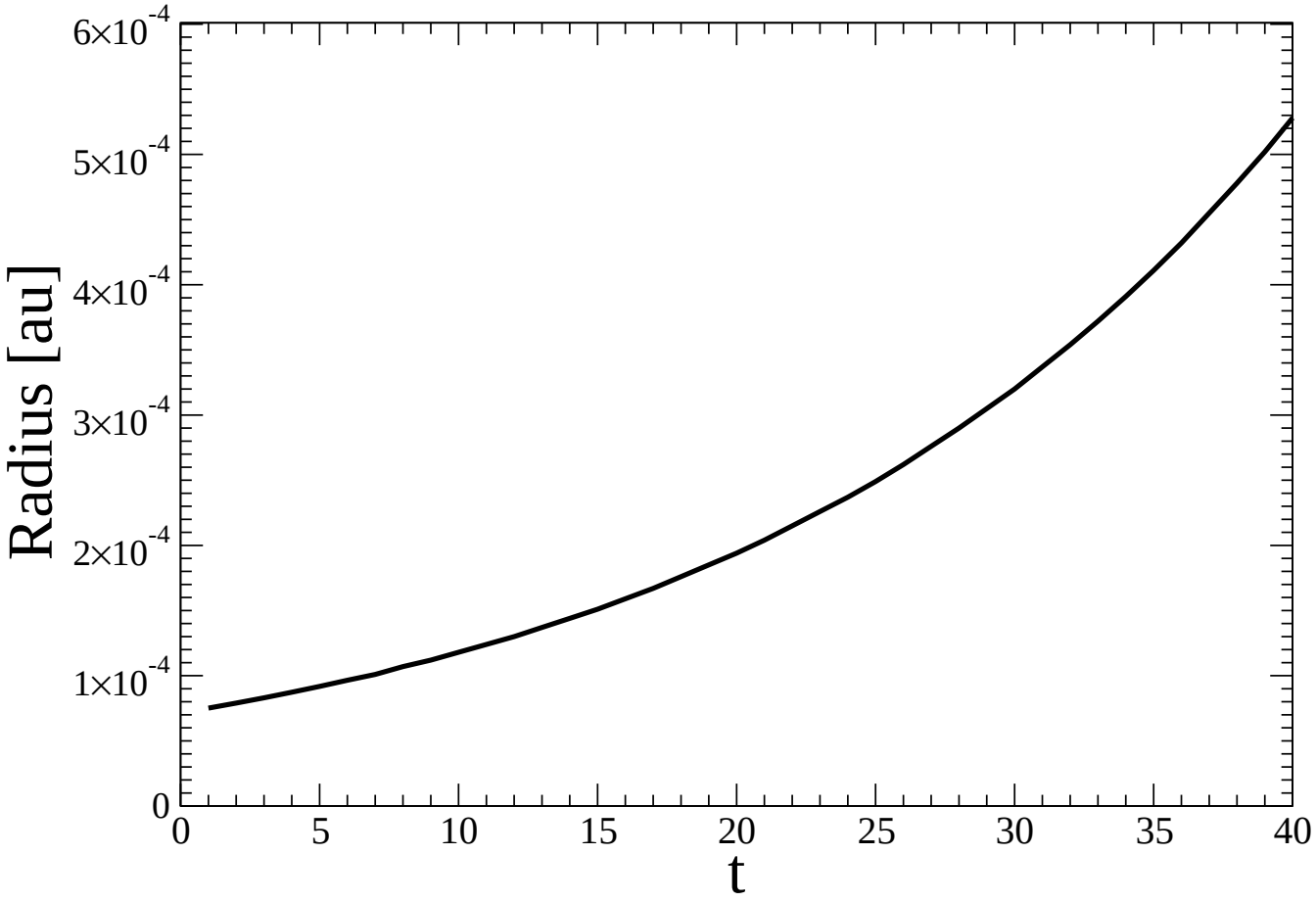

Figure 10: Radial distance in Bohr radii $[a_0]$ equal to atomic units $[au]$ as a function of the radius parameter t used in figure 9 and in eqs. (36) and (37).

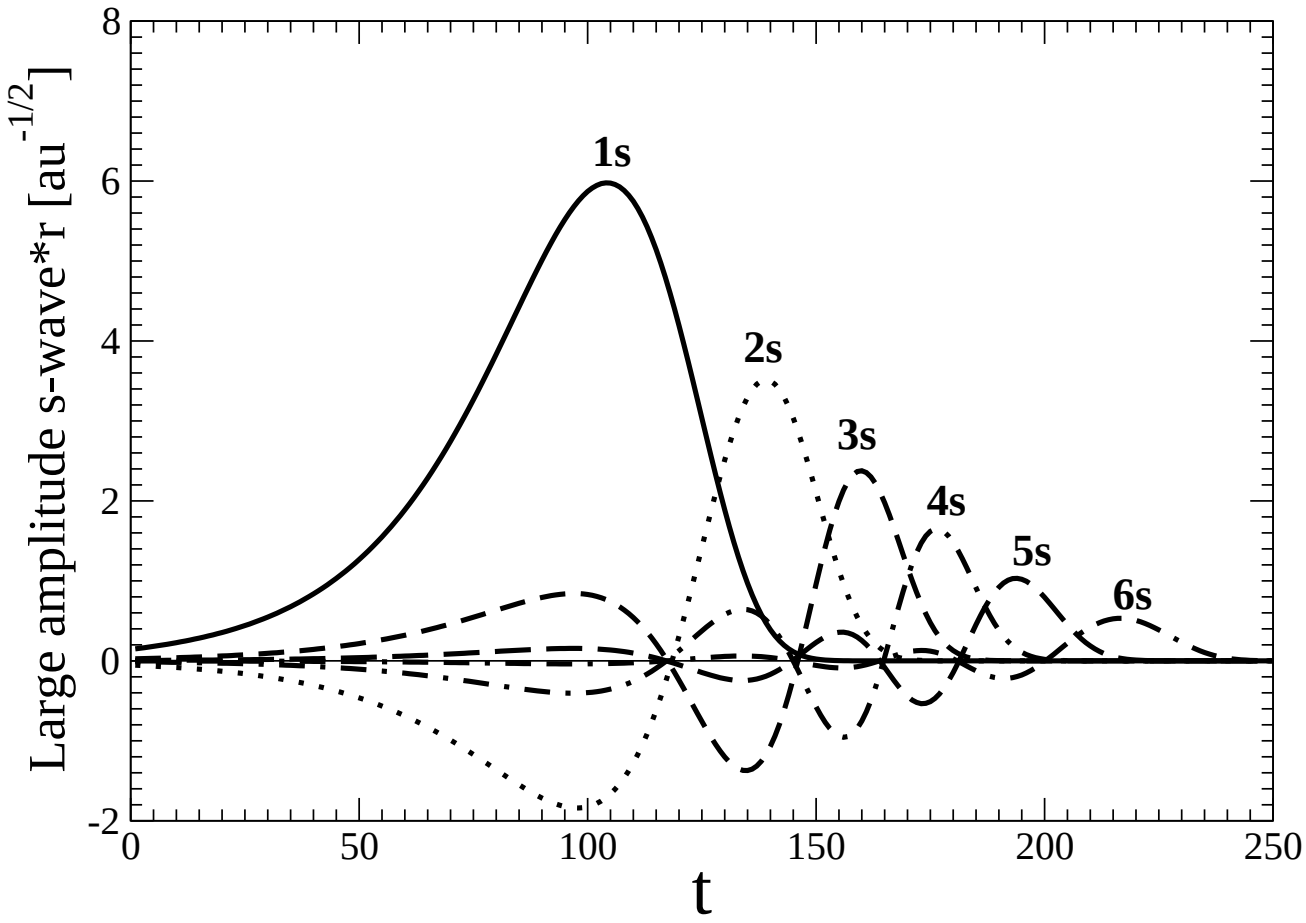

Figure 11: 1s (solid line), 2s (dotted), 3s (short-dashed), 4s (dashed-dotted) 5s (long-dashed) and 6s (dashed-dashed-dotted) normalized upper spinor amplitudes of the electron wave functions for the Holmium ground state multiplied by r as functions of the distance parameter t defined in figures (9), (10) and eqs. (36) and (37) .

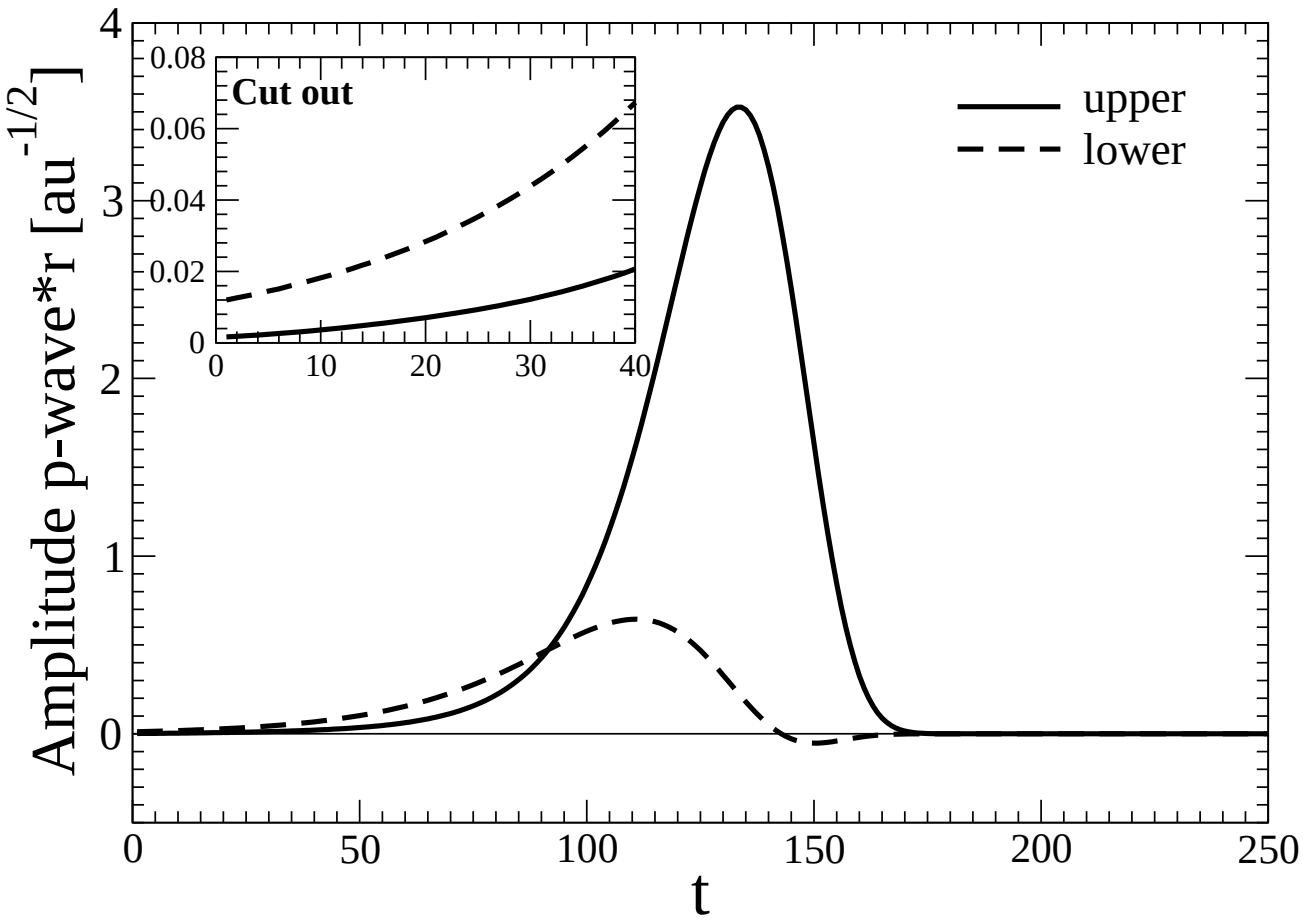

Figure 12: Normalized upper (solid line) and lower (dashed) spinor amplitudes of the Ho electron wave functions $2p_{1/2}$ multiplied by r. The cut out shows, that the lower amplitude is for small r larger then the upper amplitude as a function of the logarithmic radial parameter t definded in eqs. (36) and (37) and graphically shown in figures (9) and (10).

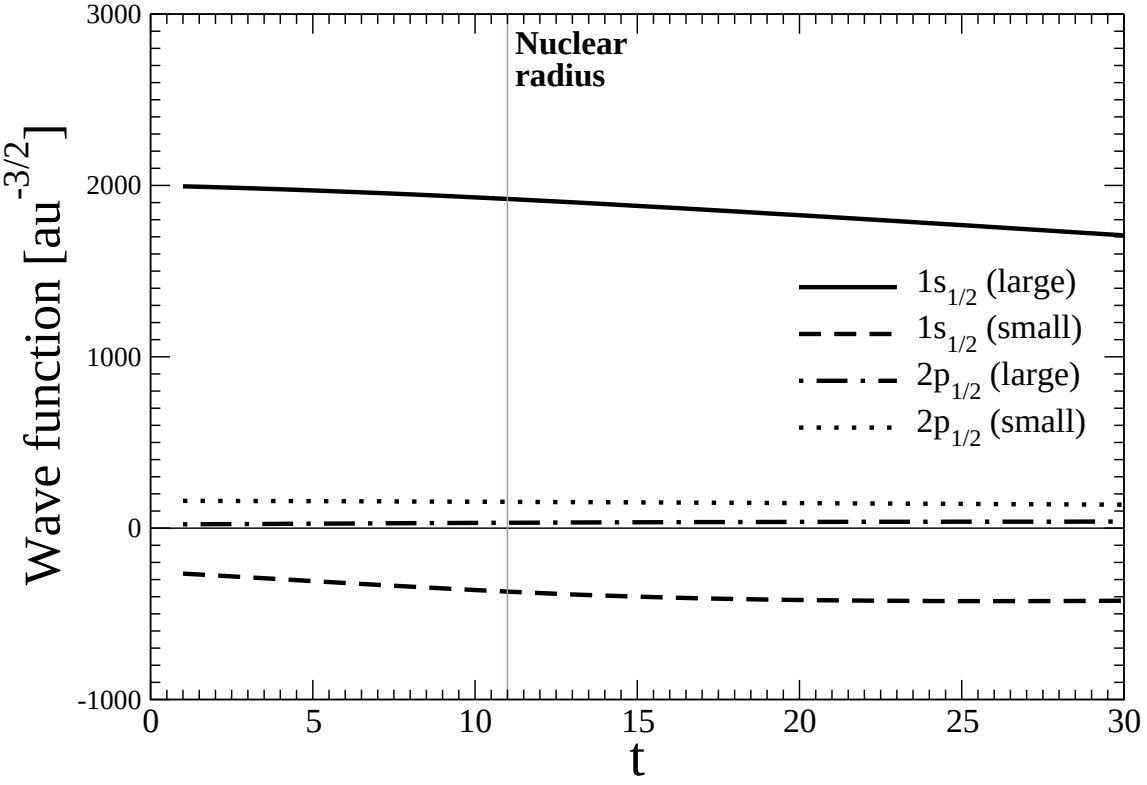

Figure 13: Normalized electron wave function not multiplied by r (9) $P(r)/r$ and $Q(r)/r$ for the $1s$ and $2p_{1/2}$ electron in Holmium 163 for the ground state configuration. The figure shows, that the lower $2p_{1/2}$ amplitude (here called 'small') is at small r larger than the upper one. The logarithmic distance parameter t is defined in eqs. (36) and (37) and graphically shown in figures (9) and (10). The nuclear radius of the Fermi distribution (11), (28) and (29) lies at $t = 11$.